

# PARALLELIZING SEQUENTIAL SWEEPING ON STRUCTURED GRIDS – FULLY PARALLEL SOR/ILU PRECONDITIONERS FOR STRUCTURED N-DIAGONAL MATRICES

R. TAVAKOLI \*

August 24, 2010

**Abstract.** There are variety of computational algorithms need sequential sweeping; sweeping based on specific order; on a structured grid, e.g., preconditioning (smoothing) by SOR or ILU methods and solution of eikonal equation by fast sweeping algorithm. Due to sequential nature, parallel implementation of these algorithms usually leads to miss of efficiency; e.g. a significant convergence rate decay. Therefore, there is an interest to parallelize sequential sweeping procedures, keeping the efficiency of the original method simultaneously. This paper goals to parallelize sequential sweeping algorithms on structured grids, with emphasis on SOR and ILU preconditioners. The presented method can be accounted as an overlapping domain decomposition method combined to a multi-frontal sweeping procedure. The implementation of method in one and two dimensions are discussed in details. The extension to higher dimensions and general structured n-diagonal matrices is outlined. Introducing notion of alternatively block upper-lower triangular matrices, the convergence theory is established in general cases. Numerical results on model problems show that, unlike related alternative parallel methods, the convergence rate and efficiency of the presented method is close to the original sequential method. Numerical results also support successful use of the presented method as a cache efficient solver in sequential computations as well.

**Key words.** domain decomposition, overlapping decomposition, parallel GaussSeidel, parallel sweeping.

**AMS subject classifications.** 65F10, 65H10, 65N06, 65N22, 65Y05

**1. Introduction.** Structured grids are commonly used in scientific computing for the purpose of numerical solution of partial differential equations (PDEs). Despite the unstructured grid based methods which manage domain complexity in a more consistent manner, in certain applications using structured grids is still the best choice, mainly due to preference in terms of consumed memory, efficiency and the ease of implementation. Moreover, with the invention of immersed boundary methods with make possible to manage complex geometries on structured grids, there is recently a significant interest to application of structured grids in scientific computing. Progress in power of supercomputer changes the bias in favor of structured grids too, as they are usually more appropriate for parallel computing.

Some of numerical algorithms on structured grids use sequential sweeping; grid by grid procedure on a mandatory order. In fact, using the conventional version of sequential algorithms, it is not possible to perform computations simultaneously. This limit us to use full power of multi-processor shared and/or distributed memory machines.

Since the advent of parallel computers, several parallel versions of the SOR method have been developed. Most variants of these algorithms have been developed by using multi-color ordering schemes or domain decomposition techniques [2, 13, 1, 17, 27, 14, 15, 5, 7, 19, 11, 23, 29]. In contrast to domain decomposition method, a multi-color SOR method has usually a faster convergence rate, but is usually more difficult to solve elliptic boundary value problems in complex domains

---

\*Department of Material Science and Engineering, Sharif University of Technology, Tehran, Iran, P.O. Box 11365-9466, email: [tav@mehr.sharif.edu](mailto:tav@mehr.sharif.edu), [rohtav@gmail.com](mailto:rohtav@gmail.com).

[28]. To improve the convergence rate of a domain decomposition algorithms, a novel mesh partition strategy was proposed in [29] which led to an efficient parallel SOR. This method has the same asymptotic rate of convergence as the Red-Black SOR [29]. Although, multi-color SOR algorithms are also usually implemented based on a domain decomposition strategy, the Xie and Adams's algorithm [29] takes less inter-processor data communication time than a multi-color SOR. The blocked version of the Xie and Adams's parallel SOR algorithm [29] is suggested in Xie [28]. According to presented results, the rate of convergence and parallel performance of this version is better than that of the non-blocked version.

The main drawback of the above mentioned parallel versions of SORs is lower rate of convergence in contrast to original one. This is mainly due to enforced decoupling between equations to provide some degree of concurrency in computations. For example in the m-color SOR method, an increase in the number of colors decreases the rate of convergence. So a key to achieve an efficient parallel SOR method is to minimize the degree of decoupling due to parallelization.

Other techniques such as the pipelining of computation and communication and an optimal schedule of a feasible number of processors are also applied to develop parallel SOR methods when the related coefficient matrix is banded [16, 20, 10, 18, 4, 3]. These techniques can isolate parts of the SOR method which can be implemented in parallel without changing the sequential SOR. The convergence rate of these methods are same as the original one but the application is limited to banded-structure matrices.

The present goals to suggest a new method to parallelize sequential sweeping on structured grids. The specific focus is on the SOR method which can be regarded as an iterative preconditioner, smoother or even a linear solver. Without loss of generality, the later case is taken into account in this study to simplify arguments. Since there is a direct correspondence between SOR and ILU preconditioners on structured grids, the presented method can be used to develop parallel ILU methods as well.

The rest of this paper is organized as follows. Sections 2 and 3 present the implementation of method in one and two spatial dimensions respectively. The extension to three spatial dimensions is commented in Section 4. he Considering the connection between SOR and ILU preconditioners on structured grids, Section 5 argues the application of presented approach to develop ILU(p) preconditioners on structured grids. The convergence theory is established in Section 6. Section 7 extend utility of the presented method to general structured n-diagonal matrices. Section 8 is devoted to numerical results on the convergence and performance of the method. Finally Section 9 close this paper by summarizing results and outlining possible application and extension of the presented method.

**2. Parallel SOR sweeping in one-dimension.** Consider the following scalar 1D elliptic PDE:

$$-\frac{d}{dx}\left(\alpha \frac{du}{dx}\right) + \beta u = f \text{ in } \Omega, \text{ and } u = u_0(x) \text{ on } \Gamma \quad (2.1)$$

where  $\Omega = [0, L_x]$ ,  $\Gamma = \partial\Omega$ ,  $\alpha : \Omega \rightarrow \mathbb{R}^+$  is  $C^1$ ,  $\beta \in \mathbb{R}^+ \cup \{0\}$ . Also, it is assumed field variables  $u$ ,  $u_0$  and  $f$  posses the sufficient regularity required by the applied numerical method to ensure the existence and uniqueness of the discrete solution. Assume the spatial domain is discrtized into an  $n + 1$  intervals with grid points  $x_i = x_{i-1} + \delta x_{i-1}$ ,  $i = 1, \dots, n$  and  $x_0 = 0$ ,  $x_{n+1} = L_x$ , where  $\delta x_i = x_{i+1} - x_i$ .

Without loss of generality; for the ease of presentation; we discretize (2.1) with a second order finite difference method as follows:

$$-c_i u_{i-1} + b_i u_i - a_i u_{i+1} = f_i, \quad i = 1, \dots, n. \quad (2.2)$$

where subscript  $i$  denotes the value of field variable at  $x = x_i$  (e.g.  $u_i = u(x_i)$ ),

$$a_i = \frac{2\alpha_{i+1/2}}{\delta x_i(\delta x_i + \delta x_{i-1})}, \quad c_i = \frac{2\alpha_{i-1/2}}{\delta x_{i-1}(\delta x_i + \delta x_{i-1})}, \quad b_i = a_i + c_i + \beta,$$

$$\alpha_{i+1/2} = \frac{2\alpha_i \alpha_{i+1}}{\alpha_i + \alpha_{i+1}}, \quad \alpha_{i-1/2} = \frac{2\alpha_i \alpha_{i-1}}{\alpha_i + \alpha_{i-1}}$$

. Using boundary conditions  $u_0 = u_0(x_0)$  and  $u_{n+1} = u_0(x_{n+1})$ , it is possible to write above equations in the following matrix form,

$$\mathbf{A}\mathbf{u} = \mathbf{f}, \quad (2.3)$$

$$A = \begin{bmatrix} b_1 & -a_1 & & & \\ -c_2 & b_2 & -a_2 & & \\ & -c_3 & \ddots & \ddots & \\ & & \ddots & \ddots & -a_{n-1} \\ & & & -c_n & b_n \end{bmatrix}_{n \times n},$$

where  $\mathbf{u} = [u_1, u_2, \dots, u_n]^T$  and  $\mathbf{f} = [c_1 u_0 + f_1, f_2, \dots, f_{n-1}, f_n + a_n u_{n+1}]^T$ . It is evident that matrix  $A$  is irreducibly diagonally dominant which ensure the convergence of stationary iterative methods, like SOR. The SOR method using the natural row-wise ordering (left to right sweeping) generates the following sequence of iterations from a given initial guess  $u_i^{(0)}$ ,

$$u_i^{(k+1)} = (1 - \omega_L)u_i^{(k)} + \frac{\omega_L}{b_i}(c_i u_{i-1}^{(k+1)} + a_i u_{i+1}^{(k)} + f_i), \quad i = 1, \dots, n, \quad (2.4)$$

where  $\omega_L \in (0, 2)$  is left to right (LR) sweeping relaxation factor and superscript  $(k)$  denotes the iteration number. The other alternative SOR method is resulted by reversing the sweeping direction (right to left sweeping):

$$u_i^{(k+1)} = (1 - \omega_R)u_i^{(k)} + \frac{\omega_R}{b_i}(c_i u_{i-1}^{(k)} + a_i u_{i+1}^{(k+1)} + f_i), \quad i = n, \dots, 1. \quad (2.5)$$

where  $\omega_R \in (0, 2)$  is the right to left (RL) sweeping relaxation factor. The application of (2.4) and (2.5) alternatively during each two consecutive iterations leads to the classical symmetric SOR (SSOR) method. It is clear that these procedures are sequential, in the sense that update of grid point  $i$  should be performed after its left (or right) neighbor. In fact, it is not possible to perform relaxation of more than one grid point at each time in the original version of SOR method.

The goal of parallel implementation of SOR method is to provide possibility of concurrent computation, simultaneously keep the convergence rate of original SOR method as much as possible. The concept of domain decomposition is used here to parallelize the SOR method. Assume spatial domain  $\Omega$  is decomposed into  $p$  number

of non-overlapping sub-domains, i.e.,  $\Omega = \cup_{i=1}^p \Omega_i$ , and  $\Omega_i \cap_{i \neq j} \Omega_j = \emptyset$ , for  $i = 1, \dots, p$  (splitting of grid points).

For the purpose of convenience, we first describe our method for two (approximately equal) sub-domains. As illustrated in figure 2.1, discretized spatial domain is decomposed into sub-domains  $\Omega_1$  and  $\Omega_2$ , where  $\Omega_1 = [0, x_m]$  and  $\Omega_2 = [x_{m+1}, L]$ . If (2.4) is used in  $\Omega_1$  and the computation begins from the left boundary, and simultaneously, (2.5) is used in  $\Omega_2$  and the calculation is performed from the right boundary toward left direction, then the computation of sub-domains will be independent during the first iteration. In our algorithm during the next iteration (2.5) and (2.4) are used respectively in  $\Omega_1$  and  $\Omega_2$ ; and the computations are started from grid points  $x_m$  and  $x_{m+1}$  in the corresponding sub-domains. Therefore, we have the following equation at grid point  $x_m$ ,

$$u_m^{(k+1)} - \frac{\omega_R a_m}{b_m} u_{m+1}^{(k+1)} = (1 - \omega_R) u_m^{(k)} + \frac{\omega_R}{b_m} (c_m u_{m-1}^{(k)} + f_m), \quad (2.6)$$

while the following equation should be used at grid point  $x_{m+1}$ ,

$$u_{m+1}^{(k+1)} - \frac{\omega_L c_{m+1}}{b_{m+1}} u_m^{(k+1)} = (1 - \omega_L) u_{m+1}^{(k)} + \frac{\omega_L}{b_{m+1}} (a_{m+1} u_{m+2}^{(k)} + f_{m+1}). \quad (2.7)$$

2.6 and (2.7) can be written in the following matrix form:

$$\begin{bmatrix} 1 & -\frac{a_m \omega_R}{b_m} \\ -\frac{c_{m+1} \omega_L}{b_{m+1}} & 1 \end{bmatrix} \begin{bmatrix} u_m^{(k+1)} \\ u_{m+1}^{(k+1)} \end{bmatrix} = \begin{bmatrix} r_m \\ r_{m+1} \end{bmatrix}, \quad (2.8)$$

$$r_m = (1 - \omega_R) u_m^{(k)} + \frac{\omega_R}{b_m} (c_m u_{m-1}^{(k)} + f_m),$$

$$r_{m+1} = (1 - \omega_L) u_{m+1}^{(k)} + \frac{\omega_L}{b_{m+1}} (a_{m+1} u_{m+2}^{(k)} + f_{m+1}).$$

The above  $2 \times 2$  system of equation can be easily inverted to compute  $u_{m+1}^{(k)}$  and  $u_m^{(k+1)}$ . Computing the new values of grid points  $x_m$  and  $x_{m+1}$  based on the mentioned procedure, the computations for the remaining grid points will be performed trivially according to the corresponding update formulae. These sequence of computation is repeated for each pair of consecutive iterations until the convergence criteria is satisfied. The flow chart of this procedure is displayed in figure 2.1. In this plot  $\oplus$  and  $\ominus$  symbols are used to denote the application of (2.4) and (2.5) respectively; also symbol  $\otimes$  is used to denote the application of (2.8).

The extension of this algorithm to more than two sub-domains is a straightforward job which can be described as follow (cf. figure 2.2):

- (i) Division of the spatial computational domain into desired number of sub-domains, based on desired load balancing constraints.
- (ii) Determination of the sweeping direction for each sub-domain. Sweeping direction of each sub-domain should be in opposite direction of its neighbors. For example we use LR direction for odd sub-domains and RL direction for even sub-domains. These sweeping directions are inverted after each iteration.
- (iii) Updating the starting node of each sub-domain with (2.8) and the remained nodes with either of (2.4) or (2.5), based on the corresponding sweeping direction. If the starting node be located at the physical boundaries, the prescribed boundary value will be used there (there is no need to use (2.8) in this case).

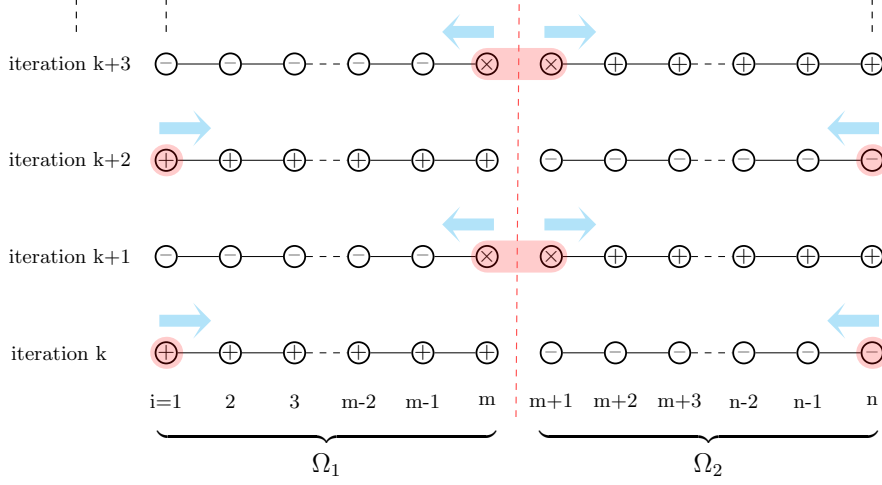


FIG. 2.1. The diagram of the parallel implementation of the presented SOR method for two sub-domains.

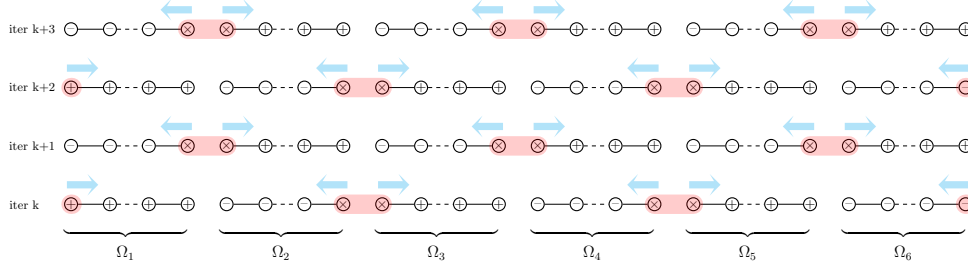


FIG. 2.2. The diagram of the parallel implementation of the presented SOR method in one-dimension for multiple number of sub-domains.

Now let's look at the properties of the presented parallel algorithm and its connection to other domain decomposition methods. It is obvious that this algorithm is an overlapping domain decomposition method which changes the overlap regions area alternatively. As the method has some similarities to overlapping Schwarz algorithm, let's mention some differences of our algorithm with the Schwarz method. In contrast to the Schwarz method the size of overlap regions here are changes alternatively. Sub-system of equations are only solved exactly at overlapped regions (of course alternatively); and within internal regions of sub-domains, equations are solved approximately (by one-pass SOR iteration). In Schwarz algorithm sub-domain boundaries are treated as virtual boundary conditions of Dirichlet, Neumann, Robin or mixture of these types. When relaxation factors are equal to unity (Gauss-Seidel iterations), our numerical treatment for sub-domain boundaries are equivalent to Neumann-type (flux) boundary conditions, in the other cases our internal boundary conditions are equivalent to a mixture of Dirichlet and Neumann ones. In the later case, the relaxation factors  $\omega_L$  and  $\omega_R$  plays role of blending factors. In fact our method tries to keep the partial coupling between sub-domain during iterations, in expense of a negligible computational cost. It is worth mentioning that due to

alteration of sweeping directions we expect good smoothing properties of the presented method. Later we will observe that how such enforced local coupling leads to competitive convergence rate of the presented method in contrast to that of original SOR.

Note that the procedure for higher order stencils or other numerical methods are conceptually the same. We avoid further remarks in this regard to save the space.

**3. Parallel SOR sweeping in two-dimensions.** In this section we shall extend the presented parallel sweeping algorithm for two-dimensional problems. We consider the following scalar 2D elliptic PDE:

$$-\nabla \cdot (\alpha \nabla u) + \beta u = f \text{ in } \Omega, \text{ and } u = u_0(x) \text{ on } \Gamma \quad (3.1)$$

where  $\Omega \in \mathbb{R}^2$ ,  $\Gamma = \partial\Omega$ ,  $\alpha : \Omega \rightarrow \mathbb{R}^{2 \times 2}$  is  $C^1$  diagonal matrix with diagonal entries  $\alpha_x, \alpha_y \in \mathbb{R}^+$ ,  $\beta \in \mathbb{R}^+ \cup \{0\}$ . For the sake of convenience, it is assumed that  $\Omega = [0, L_x] \times [0, L_y]$ . Same as previous, sufficient regularities are assumed for the field variables.

Suppose that  $\Omega$  is divided into  $(n+2)$  and  $(m+2)$  Cartesian grids along  $x$  and  $y$  directions respectively. The grid points  $(x_i, y_j)$  are given by  $x_i = x_{i-1} + \delta x_{i-1}$ ,  $i = 1, \dots, n$  and  $y_j = y_{j-1} + \delta y_{j-1}$ ,  $j = 1, \dots, m$ ; where  $x_0 = y_0 = 0$ ,  $x_{n+1} = L_x$ ,  $y_{m+1} = L_y$ ,  $\delta x_i = x_{i+1} - x_i$  and  $\delta y_j = y_{j+1} - y_j$ . Same as previous, the finite difference approximation of (3.1) is used here to describe the presented method (with second order central differencing scheme). Higher order finite difference methods as well as other numerical methods (like FVM, FEM) can also be employed. The only requirement of our method is discretization of PDE on a structured grid. We use  $w_{i,j}$  to denote the finite difference approximations of  $w(x_i, y_j)$ . The approximation of (3.1) with the mentioned scheme has the following form,

$$-a_{i,j}^S u_{i,j-1} - a_{i,j}^W u_{i-1,j} + a_{i,j}^P u_{i,j} - a_{i,j}^E u_{i+1,j} - a_{i,j}^N u_{i,j+1} = f_{i,j}, \quad (3.2)$$

for  $i = 1, \dots, n$  and  $j = 1, \dots, m$ ; where  $a_{i,j}^P = a_{i,j}^S + a_{i,j}^W + a_{i,j}^E + a_{i,j}^N + \beta$ ,

$$a_{i,j}^E = \frac{2\alpha_{xi+1/2,j}}{\delta x_i(\delta x_i + \delta x_{i-1})}, \quad a_{i,j}^W = \frac{2\alpha_{xi-1/2,j}}{\delta x_{i-1}(\delta x_i + \delta x_{i-1})},$$

$$a_{i,j}^N = \frac{2\alpha_{yi,j+1/2}}{\delta y_j(\delta y_j + \delta y_{j-1})}, \quad a_{i,j}^S = \frac{2\alpha_{yi,j-1/2}}{\delta y_{j-1}(\delta y_j + \delta y_{j-1})},$$

and the mid grid point coefficient are computed by harmonic averaging, e.g.,

$$\alpha_{xi+1/2,j} = \frac{2\alpha_{xi,j}\alpha_{xi+1,j}}{\alpha_{xi,j} + \alpha_{xi+1,j}}, \quad \alpha_{yi,j+1/2} = \frac{2\alpha_{yi,j}\alpha_{yi,j+1}}{\alpha_{yi,j} + \alpha_{yi,j+1}}.$$

Using the corresponding boundary conditions,

$$u_{0,j} = u_0(0, y_j), \quad u_{n+1,j} = u_0(x_{n+1}, y_j), \quad j = 1, \dots, m.$$

$$u_{i,0} = u_0(x_i, 0), \quad u_{i,m+1} = u_0(x_i, y_{m+1}), \quad i = 1, \dots, n.$$

Same as previous, it is possible to write above equations in a matrix form. However, the presented method is matrix-free and there is no need to write equations explicitly in a matrix form at this point.

There are variety of sweeping direction to solve (3.2) with SOR method. Considering a rectangular computational domain, it is possible to start sweeping procedure from one corner toward its corresponding opposite corner. Therefore, there is four sweep directions. Using geographic directions (east, west, north, south), it is possible to show these directions by SW-to-NE, NE-to-SW, SE-to-NW and NW-to-SE. There are various sweeping strategy for each of mentioned directions. These strategies are shown in figure 3.1 for SW-to-NE, NE-to-SW directions on a  $3 \times 3$  structured grid. Every sweeping strategy should preserve causality; should be performed along a causal direction. The causality here means that order of update should be such that new values of at least one half of neighboring nodes of the current grid should be known prior to its update. It is possible to use distinct relaxation factors along each sweeping direction. We show relaxation parameter of each direction by subscript according to its starting corner, i.e.,  $w_{SW}$ ,  $w_{NE}$ ,  $w_{SE}$ ,  $w_{NW}$ .

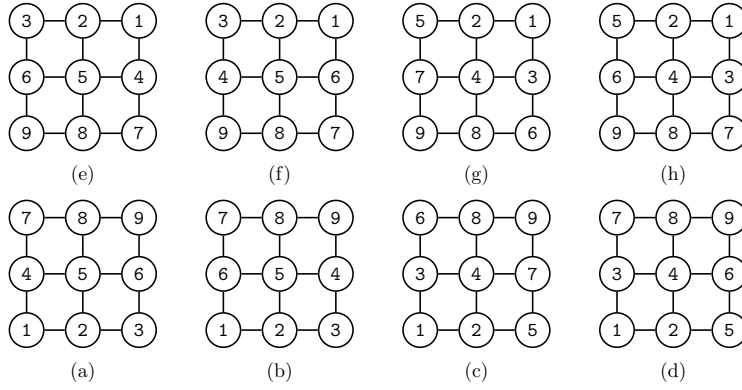


FIG. 3.1. Possible sweeping strategies for SW-to-NE (bottom row), NE-to-SW (top row) directions on a  $3 \times 3$  structured grid: order of updating procedure in natural row-wise (a, e), symmetric row-wise (b, f) and frontal (c, d, g, h) sweeping strategy.

The SOR updating (from iteration  $k$  to  $k + 1$ ) formulae for grid point  $(i, j)$  has one of the following formulae,

$$u_{i,j}^{(k+1)} = (1 - \omega_{SW})u_{i,j}^{(k)} + \frac{\omega_{SW}}{a_{i,j}^P} (a_{i,j}^S u_{i,j-1}^{(k+1)} + a_{i,j}^W u_{i-1,j}^{(k+1)} + a_{i,j}^E u_{i+1,j}^{(k)} + a_{i,j}^N u_{i,j+1}^{(k)} + f_{i,j}) \quad (3.3)$$

$$u_{i,j}^{(k+1)} = (1 - \omega_{NE})u_{i,j}^{(k)} + \frac{\omega_{NE}}{a_{i,j}^P} (a_{i,j}^S u_{i,j-1}^{(k)} + a_{i,j}^W u_{i-1,j}^{(k)} + a_{i,j}^E u_{i+1,j}^{(k+1)} + a_{i,j}^N u_{i,j+1}^{(k+1)} + f_{i,j}) \quad (3.4)$$

$$u_{i,j}^{(k+1)} = (1 - \omega_{SE})u_{i,j}^{(k)} + \frac{\omega_{SE}}{a_{i,j}^P} (a_{i,j}^S u_{i,j-1}^{(k+1)} + a_{i,j}^W u_{i-1,j}^{(k)} + a_{i,j}^E u_{i+1,j}^{(k+1)} + a_{i,j}^N u_{i,j+1}^{(k)} + f_{i,j}) \quad (3.5)$$

$$u_{i,j}^{(k+1)} = (1 - \omega_{NW})u_{i,j}^{(k)} + \frac{\omega_{NW}}{a_{i,j}^P} (a_{i,j}^S u_{i,j-1}^{(k)} + a_{i,j}^W u_{i-1,j}^{(k+1)} + a_{i,j}^E u_{i+1,j}^{(k)} + a_{i,j}^N u_{i,j+1}^{(k+1)} + f_{i,j}) \quad (3.6)$$

It is clear that due to required causality condition, the above procedures are sequential in nature. To parallelize this sequential procedure, we first split the computational domain into  $p$  (almost) equally-size non-overlapping sub-domains (based

on load balancing constraints). To describe our algorithm, we consider a Cartesian decomposition in this section, i.e.,  $p = p_x \times p_y$  where  $p_x$  along  $p_y$  are number of sub-domains along  $x$  and  $y$  spatial axes respectively. For the sake of convenience, it is assumed that  $\Omega$  is decomposed into a  $2 \times 2$  array of sub-domains (cf. figure 3.2).

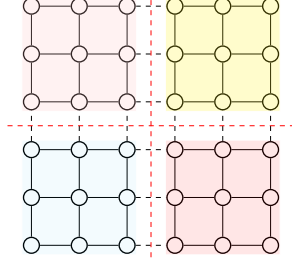


FIG. 3.2. Decomposition of a  $6 \times 6$  Cartesian mesh into  $2 \times 2$  array of sub-domains.

As it is implied in previous, a key to achieve a parallel SOR with a little convergence rate decay is to minimize degree of decoupling due to parallelizing, as much as possible. In the original SOR when a point is updated the remaining points sense its new value due to causality of sweeping strategy.

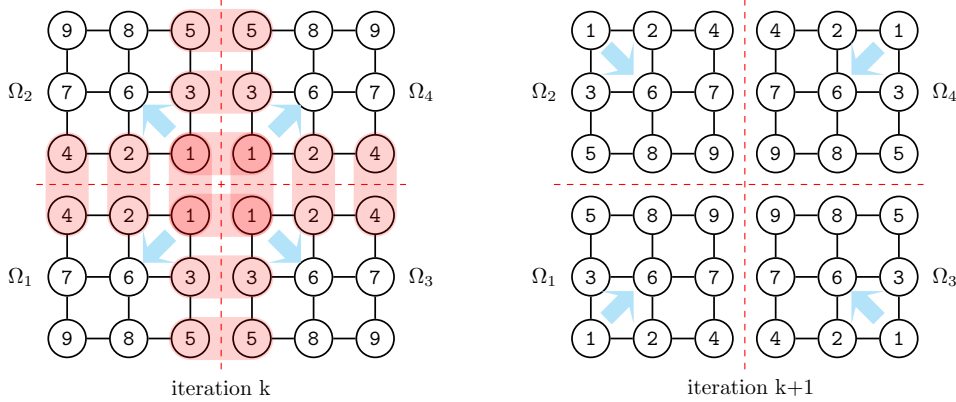


FIG. 3.3. Decomposition of a  $6 \times 6$  Cartesian mesh into  $2 \times 2$  array of sub-domains: sweeping directions and order of update are shown during two consecutive iterations, coupling between nodes are shown by shading.

To keep the causality of sweeping partially, a multi-frontal strategy is employed here for the purpose of parallelization. Consider the mentioned  $2 \times 2$  Cartesian splitting of the computational domain. According to figure 3.3, we use frontal sweeping along directions,  $NE$ ,  $NW$ ,  $SE$  and  $SW$  for sub-domains 1 though 4 respectively. The order of updating is shown in plots. It is clear that to update node #1 of each sub-domain, we need two unknown values (new values) from two neighbor sub-domains. A shaded region in figure show this coupling in iteration  $k$ -th. Therefore a local  $4 \times 4$  system of equation should be solved for this purpose. Assuming node #1 of  $\Omega_1$  (at iteration  $k$ -th, left side of figure) is denoted by  $(i, j)$  and using global index, this local system of equation has the following form (application of (3.4), (3.6), (3.5) and (3.3))



for  $\Omega_1$  though  $\Omega_4$  respectively),

$$\begin{bmatrix}
1 & -\frac{\omega_{NE}a_{i,j}^E}{a_{i,j}^P} & -\frac{\omega_{NE}a_{i,j}^N}{a_{i,j}^P} & 0 \\
-\frac{\omega_{NW}a_{i+1,j}^W}{a_{i+1,j}^P} & 1 & 0 & -\frac{\omega_{NW}a_{i+1,j}^N}{a_{i+1,j}^P} \\
-\frac{\omega_{SE}a_{i,j+1}^S}{a_{i,j+1}^P} & 0 & 1 & -\frac{\omega_{SE}a_{i,j+1}^E}{a_{i,j+1}^P} \\
0 & -\frac{\omega_{SW}a_{i+1,j+1}^S}{a_{i+1,j+1}^P} & -\frac{\omega_{SW}a_{i+1,j+1}^W}{a_{i+1,j+1}^P} & 1
\end{bmatrix}
\begin{bmatrix}
u_{i,j}^{(k+1)} \\
u_{i+1,j}^{(k+1)} \\
u_{i,j+1}^{(k+1)} \\
u_{i+1,j+1}^{(k+1)}
\end{bmatrix} =
\begin{bmatrix}
(1 - \omega_{NE})u_{i,j}^{(k)} + \frac{\omega_{NE}(a_{i,j}^S u_{i,j-1}^{(k)} + a_{i,j}^W u_{i-1,j}^{(k)} + f_{i,j})}{a_{i,j}^P} \\
(1 - \omega_{NW})u_{i+1,j}^{(k)} + \frac{\omega_{NW}(a_{i+1,j}^S u_{i+1,j-1}^{(k)} + a_{i+1,j}^E u_{i+2,j}^{(k)} + f_{i+1,j})}{a_{i+1,j}^P} \\
(1 - \omega_{SE})u_{i,j+1}^{(k)} + \frac{\omega_{SE}(a_{i,j+1}^W u_{i-1,j+1}^{(k)} + a_{i,j+1}^N u_{i,j+2}^{(k)} + f_{i,j+1})}{a_{i,j+1}^P} \\
(1 - \omega_{SW})u_{i+1,j+1}^{(k)} + \frac{\omega_{SW}(a_{i+1,j+1}^E u_{i+2,j+1}^{(k)} + a_{i+1,j+1}^S u_{i+1,j+2}^{(k)} + f_{i+1,j+1})}{a_{i+1,j+1}^P}
\end{bmatrix} \quad (3.7)$$

This system of equation is non-singular and can be easily inverted. After update of the corner node (node 1), we should update nodes on (virtual) boundaries of sub-domains. As it is shown in figure 3.3, node #2 of each sub-domain is coupled to node #2 of a neighbor sub-domain. Assuming node #1 of  $\Omega_1$  is denoted by  $(i, j)$  and using global index, using (3.4) and (3.5) the following  $2 \times 2$  system of equations should be solved to compute new values of node #2 in  $\Omega_1$  and  $\Omega_3$ , in fact  $(i-1, j)$  and  $(i-1, j+1)$  (cf. 3.3),

$$\begin{bmatrix}
1 & -\frac{\omega_{NE}a_{i-1,j}^N}{a_{i-1,j}^P} \\
-\frac{\omega_{SE}a_{i-1,j+1}^S}{a_{i-1,j+1}^P} & 1
\end{bmatrix}
\begin{bmatrix}
u_{i-1,j}^{(k+1)} \\
u_{i-1,j+1}^{(k+1)}
\end{bmatrix} =
\begin{bmatrix}
(1 - \omega_{NE})u_{i-1,j}^{(k)} + \frac{\omega_{NE}(a_{i-1,j}^S u_{i-1,j-1}^{(k)} + a_{i-1,j}^W u_{i-2,j}^{(k)} + a_{i-1,j}^E u_{i,j}^{(k+1)})}{a_{i-1,j}^P} \\
(1 - \omega_{SE})u_{i-1,j+1}^{(k)} + \frac{\omega_{SE}(a_{i-1,j+1}^W u_{i-2,j+1}^{(k)} + a_{i-1,j+1}^E u_{i,j+1}^{(k+1)} + a_{i-1,j+1}^S u_{i-1,j+2}^{(k)})}{a_{i-1,j+1}^P}
\end{bmatrix} \quad (3.8)$$

Note that the new values of  $u_{i,j}^{(k+1)}$  and  $u_{i,j+1}^{(k+1)}$  are located in right hand side of (3.8) as they are known after solution of (3.7). In the same manner other remaining boundary nodes will be updated. Then, the internal nodes will be updated using a classic SOR method along the corresponding sweeping direction.

The next sweep (iteration  $(k+1)$ -th) for the mentioned decomposition will be performed along the corresponding opposite directions, i.e.,  $SW$ ,  $SE$ ,  $NW$  and  $NE$  for sub-domains 1 though 4 respectively (cf. figure 3.3). In this specific example there is no need to solution some local system of equations for this sweep; but in general one may usually needs to solve such systems at coupling points of sub-domains which are

determined based on sweeping directions. Figure 3.4 shows the alteration of sweeping directions during each four consecutive iterations for a  $4 \times 4$  array of sub-domains. In the next following sub-sections some implementation issues of our algorithm will be discussed in details.

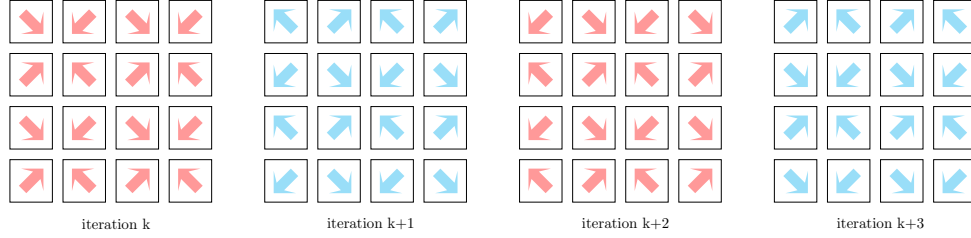


FIG. 3.4. Alternation of sweeping directions during 4 consecutive iterations for  $4 \times 4$  array of sub-domains.

As a final remark in this section it should be mentioned that the extension of our algorithm for nine-point or higher order central stencils is straightforward. As the extend of computational molecule is increased in a higher order method, the size of local systems to be solved will be also increased accordingly. Following the same strategy, it would be possible to apply the presented method for other numerical methods, e.g., FVM and FEM methods, on a structured grid. Note that every structured grid has a one-to-one correspondence with with a Cartesian grid. Therefore, the presented method can be directly used for non-Cartesian structured grids too. To save the space, further details in this regards are ignored in this study.

**3.0.1. Domain decomposition.** The first aspect of our parallel algorithm is to divide the computational grid into parts. This is how the full computational task is divided among the various processors. Each processor works on a portion of the grid and anytime a processor needs information from another one a message will be passed (in message passing protocol; no message passing is needed regarding to shared-memory machines).

To achieve a good parallel performance, we like to have an optimal load balancing and the least communication between processors. Consider the load balancing first. Assuming a homogeneous parallel machine, one would like that each processor does the same amount of work during every iteration. That way, each processor is always working and not sitting idle. It makes sense to partition the grid such that each processor gets an equal (or nearly equal) number of nodes to work on. The second criterion, needs to minimize the number of edge cuts and the degree of adjacency for each sub-domain (number of neighbors processor). So the domain decomposition could be converted to a constrained optimization problem in which the communication cost to be minimized under the load balancing constraint. In the case of regular Cartesian grid, this optimization problem can be easily solved within a negligible cost.

The cost of communication is composed from two types of elapsed time, one proportional to the communicated data size (function of network communication speed) and one due to the network latency which is independent from the data size. Therefore, dealing with a high latency networks, we may prefer to decrease the degree of adjacency in our communication graph; in expense of a higher size of communicated data size. On the other hand, dealing with low latency networks, we may neglect the effect of network latency. It is worth mentioning that, using an overlapped communi-

cation and computation strategy, it will be possible to decrease cost of communication.

The above discussion is correct in general for every parallel algorithms. However, one should consider other criteria when the convergence rate of the parallel algorithm is a function domain decomposition topology (number of sub-domains and their geometries).

In the present study increasing number of sub-domains along each spatial direction is equivalent to decreasing the degree of coupling in that direction. Rough speaking, it usually decreases the convergence rate. However, this conclusion is not correct in general. In some cases, a limited degree of decoupling not only decreases the convergence rate but also improves it. As an example consider the solution of Poisson equation in a square domain. Also, assume that the center of domain is the center of symmetry for the exact solution. Now, let's to decompose the domain into  $2 \times 2$  equal sub-domains. Due to mentioned symmetry, the parallel algorithm performs superior than the original SOR method (as it is more consistent to mentioned symmetry in actual solution). This example implies that decoupling does not always decrease the convergence rate. Therefore, one may expect that an algorithm with partial coupling (like that of ours) performs even superior than the original SOR in practice.

**3.0.2. Sweeping directions.** After the domain decomposition, it is essential to determine the sweeping directions for each sub-domain during 4 consecutive iterations. For this purpose it is sufficient to use the following rules (lie 1D version of algorithm):

- Along each spatial direction the sweeping direction of a sub-domain should be in opposite direction of its neighbor sub-domains (cf. figure 3.4).
- The sweeping directions (along all spatial directions) should be reversed during every pair of iterations (cf. figure 3.4).
- After each pair of iteration, the sweeping will be performed along a new diagonal, e.g., after two consecutive iterations along diagonal *SW-NE*, the direction of sweeping for the next two iteration will be changed to *SE-NW* diagonal (cf. figure 3.4).

Using the above mentioned rules, the sweeping directions are generated automatically without any complexity, e.g., figure 3.4 is produced applying the above mentioned rules within a nested loop using a few lines of Tikz<sup>1</sup> scripts.

**3.0.3. Data structure.** In the sequential SOR a two-dimensional array is sufficient to store the global data. This needs a nested loop to sweep the hole domain. Since in the presented parallel SOR method, we do not have a regular order of updating for sub-domains boundary nodes, it is preferable to store order of update for these nodes. To achieve better performance every data (mentioned indexes and field variables) are stored in a one-dimensional array (sometimes called as vectorization). In fact in this way we have a one-to-one mapping from 2D indexing to 1D indexing, e.g., node  $(i, j)$  is stored at location  $i + j * (n + 2)$  in the one-dimensional array. In this way, the location of nodes  $(i + 1, j)$  and  $(i, j + 1)$  will be the location of node  $(i, j)$  plus 1 and  $(n + 2)$  values respectively.

To update nodes which are located at boundaries between neighbor sub-domains, the data from the corresponding neighbor sub-domains is required. Therefore, we add two rows/columns of halo points around each sub-domain which are renewed (via

---

<sup>1</sup>[www.texample.net/tikz/](http://www.texample.net/tikz/)

communication) prior to a new iteration (in the case of higher order schemes, the width of halo region should be increased accordingly). In the present implementation every sub-domain has at most 8 neighbors, i.e., 4 first-degree neighbors (contacted via an edge), 4 second-degree neighbors (contacted via a corner). Figure 3.5 shows schematically the communicated data during *SW to NE* and *NE to SW* sweeps for a sub-domain with 8 active neighbors. In this figure, yellow-shaded regions contain native nodes and gray-shaded regions includes required data which should be communicated. It is clear that it is possible to overlap a portion of communications with computations to improve the performance.

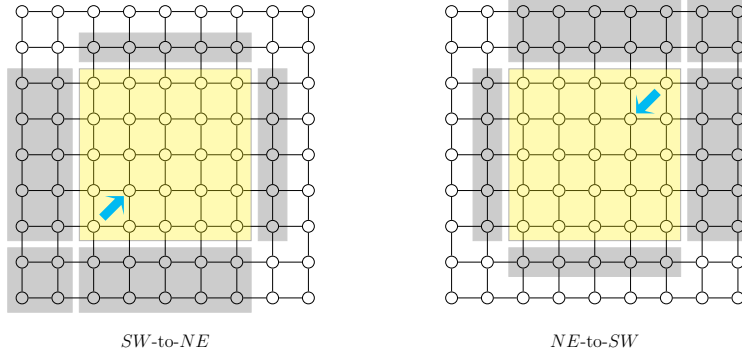


FIG. 3.5. Schematic of data communication during frontal sweeping *SW to NE* (left) and *NE to SW* (right) for a sub-domain with 8 active neighbors: yellow shaded regions contain native nodes and gray shaded regions include communicated nodes.

**4. Extension to three-dimensions.** Following the geometric procedure discussed in the previous section, it is straightforward to extend the presented method to three-dimensional (3D) cases. The main ingredients of such extensions are briefly addressed here.

In 3D case, there are eight alternatives frontal sweeping directions. Adding front and back directions to mentioned geographic directions (east, west, north, south), these eight sweep directions are as follows: *BSW-to-FNE*, *FNE-to-BSW*, *BNE-to-FSW*, *FSW-to-BNE*, *BNW-to-FSE*, *FSE-to-BNW*, *BSE-to-FNW* and *FNW-to-BSE*. There are eight relaxation parameters accordingly,  $\omega_{BSW}$ ,  $\omega_{FNE}$ ,  $\omega_{BNE}$ ,  $\omega_{FSW}$ ,  $\omega_{BNW}$ ,  $\omega_{FSE}$ ,  $\omega_{BSE}$  and  $\omega_{FNW}$ . After the domain decomposition, the sweeping directions are determined for each domain for each eight consecutive iterations using mentioned rules in 3.0.2. Using a Cartesian decomposition topology, each sub-domain will have at most 26 neighbors, i.e., 6 first-degree neighbors (contacted via a face), 12 second-degree neighbors (contacted via an edge), 8 third-degree neighbors (contacted via a corner).

Same as 2D version of algorithm, some local system of equations are needed to be solved at sub-domains coupling nodes. Now, consider a sub-domain with 26 active neighbor. At starting corner, a  $8 \times 8$  system of linear equations should be solved. Note that this system is not dense (includes 32 none-zero entries). Then, along each of the three coupling edges, a sort of  $4 \times 4$  local system of linear equations should be solved in an appropriate order. In the same manner, on each of the three corresponding coupling faces a sort of  $2 \times 2$  local systems of equations should be solved based on an appropriate update order. Updating coupling nodes, the remaining nodes are updated using classic SOR method along the corresponding sweep direction.

**5. Parallel incomplete LU preconditioners.** The SOR method does not usually used as an iterative solver in practice. But it is commonly used as a smoother in multi-grid methods or as a preconditioner in Krylov subspace methods. In these cases, a few iterations of SOR method is applied during each step of preconditioning (or smoothing). Another kind of preconditioners which are extensively used in Krylov subspace methods are incomplete LU (ILU) preconditioners. However due to sequential nature of incomplete factorization and also forward/backward substitution procedure, application of ILU methods in parallel is challenge.

In this section, we show that the presented parallel method can be equivalently used to develop parallel ILU preconditioners. A simple observation shows that single pass of a symmetric Gauss-Seidel method on a  $n$ -diagonal matrix (precisely a matrix includes only a few non-zero diagonals with symmetric sparsity pattern) is equivalent to ILU(0) preconditioning (cf. section 10.3 of [21]). Therefore, the presented parallel algorithm can be used as a parallel ILU(0) preconditioner as well. Similarly, ILU(p) preconditioning for such structured matrices is equivalent to application of our method for a higher order method (cf. section 10.3 of [21]) which make sense to use our method to parallelize ILU(p) preconditioners as well.

Later, we will show that our method can be applied for  $n$ -diagonal matrices raised from discretization of PDEs on structured grids. Therefore, the presented strategy can be also regarded as a parallel ILU(p) preconditioner for such  $n$ -diagonal matrices.

**6. Convergence analysis.** In this section we first proof the convergence of the presented parallel algorithm in one- and two- spatial dimensions. Following the same line of proof, the extension of theory to higher dimension will be straightforward.

**6.1. Mono-dimensional convergence analysis.** To simplify the analysis, it is worth to write the presented method in an algebraic form. Without loss of generality, assume that the spatial domain is decomposed into  $p$  number of sub-domains where  $p$  is an even integer and all sub-domains include  $l$  number of grid points (note that boundary nodes are not considered here, i.e.,  $n = pl$ ). Also, assume that the sweeping direction of the first sub-domain is  $LR$  at the starting iteration. We can decompose matrix  $A$  in (2.3) as follows,

$$A = G_L + \beta I + G_R, \quad (6.1)$$

where  $I$  denotes an  $n \times n$  identity matrix here,

$$G_L = \begin{bmatrix} L_1 & & & & \\ & R_2 & & & \\ & & \ddots & & \\ & & & L_{p-1} & \\ & & & & R_p \end{bmatrix}, \quad G_R = \begin{bmatrix} R_1 & & & & \\ & L_2 & & & \\ & & \ddots & & \\ & & & R_{p-1} & \\ & & & & L_p \end{bmatrix},$$

for  $q = 2, 3, \dots, p$ ,

$$L_q = \begin{bmatrix} -c_{(q-1)l+1} & c_{(q-1)l+1} & & & \\ & -c_{(q-1)l+2} & c_{(q-1)l+1} & & \\ & & \ddots & \ddots & \\ & & & -c_{ql-1} & c_{ql-1} \\ & & & & -c_{ql} & c_{ql} \end{bmatrix}_{l \times (l+1)},$$

for  $q = 1, 2, \dots, p-1$ ,

$$R_q = \begin{bmatrix} a_{(q-1)l+1} & -a_{(q-1)l+1} & & & & \\ & a_{(q-1)l+2} & -a_{(q-1)l+2} & & & \\ & & \ddots & \ddots & & \\ & & & a_{ql-1} & -a_{ql-1} & \\ & & & & a_{ql} & -a_{ql} \end{bmatrix}_{l \times (l+1)},$$

$$L_1 = \begin{bmatrix} c_1 & & & & \\ & \ddots & & & \\ & & \ddots & & \\ & & & c_{l-1} & \\ & & & -c_l & c_l \end{bmatrix}_{l \times l}, R_p = \begin{bmatrix} a_{n-l+1} & -a_{n-l+1} & & & \\ & a_{n-l+2} & \ddots & & \\ & & \ddots & & \\ & & & \ddots & -a_{n-1} \\ & & & & a_n \end{bmatrix}_{l \times l},$$

Note that matrices  $L_q$  and  $R_q$  should be assembled in  $G_L$  and  $G_R$  such that their positive diagonal match to the main diagonal of  $G_L$  and  $G_R$ . Assume that eigenvalues of matrices  $G_L$  and  $G_R$  are denoted by vectors  $\Lambda_L = [\lambda_1^l, \lambda_2^l, \dots, \lambda_n^l]^T$  and  $\Lambda_R = [\lambda_1^r, \lambda_2^r, \dots, \lambda_n^r]^T$  respectively. The following Lemma determines  $\Lambda_L$  and  $\Lambda_R$  explicitly.

LEMMA 6.1.  $G_L$  and  $G_R$  are strictly positive definite and we have,

$$\Lambda_L = [c_1, \dots, c_l, a_{l+1}, \dots, a_{2l}, \dots, c_{(p-2)l+1}, \dots, c_{(p-1)l}, a_{n-l+1}, \dots, a_n]^T$$

$$\Lambda_R = [a_1, \dots, a_l, c_{l+1}, \dots, c_{2l}, \dots, a_{(p-2)l+1}, \dots, a_{(p-1)l}, c_{n-l+1}, \dots, c_n]^T$$

*Proof.* Considering the structures of  $G_L$  and  $G_R$ , it is easy to verify that  $G_L$  and  $G_R$  are block lower and upper triangular matrices. Note that the definition of both of the block lower triangular and upper triangular matrix hold for each of  $G_L$  and  $G_R$ . Therefore, their corresponding eigenvalues are equal to union of their diagonal blocks's eigenvalues. The Diagonal blocks have a simple bi-diagonal structure and their eigenvalues are equal to their main diagonals. Considering the fact that that  $a_i, c_i > 0$ ,  $i = 1, \dots, n$  completes the proof.  $\square$

THEOREM 6.2. The presented parallel one-dimensional algorithm is convergent if  $|1 - \omega_L| |1 - \omega_R| < 1$ .

*Proof.* Considering the decomposition (6.1) of matrix  $A$ , with simple algebra, we can write the presented one-dimensional parallel iterative algorithm in the following matrix form ( $k = 0, 2, \dots$ ),

$$\begin{aligned} ((\mathbf{b} - \omega_L \Lambda_L)I + \omega_L G_L) \mathbf{u}^{(k+1)} &= (((1 - \omega_L)\mathbf{b} + \omega_L \Lambda_R)I - \omega_L G_R) \mathbf{u}^{(k)} + \omega_L \mathbf{f} \\ ((\mathbf{b} - \omega_R \Lambda_R)I + \omega_R G_R) \mathbf{u}^{(k+2)} &= (((1 - \omega_R)\mathbf{b} + \omega_R \Lambda_L)I - \omega_R G_L) \mathbf{u}^{(k+1)} + \omega_R \mathbf{f}, \end{aligned} \quad (6.2)$$

where  $\mathbf{b} \stackrel{\text{def}}{=} [b_1, b_2, \dots, b_n]^T$ . From (6.2) we have,

$$\mathbf{u}^{(k+2)} = T \mathbf{u}^{(k)} + \bar{\mathbf{f}}, \quad k = 0, 2, \dots \quad (6.3)$$

in which,

$$T = \left( (\mathbf{b} - \omega_R \Lambda_R) I + \omega_R G_R \right)^{-1} \left( ((1 - \omega_R) \mathbf{b} + \omega_R \Lambda_L) I - \omega_R G_L \right) \\ \times \left( (\mathbf{b} - \omega_L \Lambda_L) I + \omega_L G_L \right)^{-1} \left( ((1 - \omega_L) \mathbf{b} + \omega_L \Lambda_R) I - \omega_L G_R \right) \quad (6.4)$$

To proof the convergence of iterations (6.3) it is remained to show that the spectral radius of iteration matrix  $T$  which is denoted by  $\rho(T)$  here is strictly less than unity (cf. [21]). Now, let's to define the matrix  $\tilde{T}$  which is equivalent to  $T$  (has the same spectral radius),

$$\tilde{T} = \left( (\mathbf{b} - \omega_R \Lambda_R) I + \omega_R G_R \right) T \left( (\mathbf{b} - \omega_R \Lambda_R) I + \omega_R G_R \right)^{-1} \quad (6.5)$$

Using (6.4),  $\tilde{T}$  can be written as follows,

$$\tilde{T} = \left( ((1 - \omega_R) \mathbf{b} + \omega_R \Lambda_L) I - \omega_R G_L \right) \left( (\mathbf{b} - \omega_L \Lambda_L) I + \omega_L G_L \right)^{-1} \\ \times \left( ((1 - \omega_L) \mathbf{b} + \omega_L \Lambda_R) I - \omega_L G_R \right) \left( (\mathbf{b} - \omega_R \Lambda_R) I + \omega_R G_R \right)^{-1} \quad (6.6)$$

Let's to define the following matrices

$$G_{L-} = ((1 - \omega_R) \mathbf{b} + \omega_R \Lambda_L) I - \omega_R G_L, \quad G_{L+} = (\mathbf{b} - \omega_L \Lambda_L) I + \omega_L G_L$$

$$G_{R-} = ((1 - \omega_L) \mathbf{b} + \omega_L \Lambda_R) I - \omega_L G_R, \quad G_{R+} = (\mathbf{b} - \omega_R \Lambda_R) I + \omega_R G_R$$

Assume eigenvalues of  $G_{L-}$ ,  $G_{L+}$ ,  $G_{R-}$  and  $G_{R+}$  are denoted by the following vectors respectively,

$$\Lambda_{L-} = [\lambda_1^{l-}, \dots, \lambda_n^{l-}]^T, \quad \Lambda_{L+} = [\lambda_1^{l+}, \dots, \lambda_n^{l+}]^T,$$

$$\Lambda_{R-} = [\lambda_1^{r-}, \dots, \lambda_n^{r-}]^T, \quad \Lambda_{R+} = [\lambda_1^{r+}, \dots, \lambda_n^{r+}]^T,$$

It is easy to show that,

$$\Lambda_{L-} = (1 - \omega_R) \mathbf{b}, \quad \Lambda_{L+} = \mathbf{b}, \quad \Lambda_{R-} = (1 - \omega_L) \mathbf{b}, \quad \Lambda_{R+} = \mathbf{b}.$$

Using the knowledge of linear algebra we have,

$$\rho(T) = \rho(\tilde{T}) = \|\tilde{T}\| \leq \| (G_{L-}) (G_{L+}^{-1}) \| \times \| (G_{R-}) (G_{R+}^{-1}) \|$$

where the norm operator  $\|\cdot\|$  is understood as the Euclidean norm here,

$$\| (G_{L-}) (G_{L+}^{-1}) \| = \max_{1 \leq i \leq n} \left| \frac{\lambda_i^{l-}}{\lambda_i^{l+}} \right| = \max_{1 \leq i \leq n} \left| \frac{(1 - \omega_R) b_i}{b_i} \right| = |1 - \omega_R|$$

$$\| (G_{R-}) (G_{R+}^{-1}) \| = \max_{1 \leq i \leq n} \left| \frac{\lambda_i^{r-}}{\lambda_i^{r+}} \right| = \max_{1 \leq i \leq n} \left| \frac{(1 - \omega_L) b_i}{b_i} \right| = |1 - \omega_L|$$

Therefore, if,

$$|1 - \omega_L| |1 - \omega_R| < 1.$$

$\rho(T) < 1$  which complete the proof.  $\square$

**COROLLARY 6.3.** *The presented one-dimensional parallel Gauss-Seidel algorithm ( $\omega_L = \omega_R = 1$ ) is unconditionally convergent.*

**COROLLARY 6.4.** *When  $\omega_L = \omega_R = \omega$  the convergence criterion of the presented one-dimensional parallel SOR algorithm is similar to that of sequential SOR method, i.e.,  $0 < \omega < 2$ . Moreover  $\omega_{opt} = 1$  in this case.*

**REMARK 6.5.** *Using the same procedure, it will easy to show that the coefficient matrix  $A$  corresponding to a high order methods (includes more extended computational molecules) admits a decomposition like to (6.1), where  $G_L$  and  $G_R$  are two strictly positive definite block lower and upper triangular matrices respectively. Then, it will be straightforward to proof the convergence similarly.*

**6.2. Two-dimensional convergence analysis.** Following the previous section, it is possible to proof the convergence of the presented method in two spatial dimensions. To illustrate this issue, the convergence of the presented two-dimensional algorithm for discretized equation (3.2) will be discussed in this section.

Extension of mono-dimensional proof to higher dimensions is based on tensor product properties of the structured grids. The standard five-point discretization of (3.1) problem on an  $n \times m$  structured grid (ignoring Dirichlet boundary nodes) leads to the following system of linear equation (the effects of Dirichlet boundary nodes are included in the right hand side vector),

$$A\mathbf{u} = \mathbf{f}$$

where strictly positive definite  $nm \times nm$  dimensional matrix  $A$  has the following structure (row-wise ordering is assumed for grid points),

$$A = \begin{bmatrix} B_1 & A_1 & & & \\ C_2 & B_2 & A_2 & & \\ & C_3 & \ddots & \ddots & \\ & & \ddots & \ddots & A_{m-1} \\ & & & C_m & B_m \end{bmatrix}_{m \times m},$$

where each of  $B_i$ ,  $A_i$  and  $C_i$  is an  $n \times n$  multi-diagonal (three or mono-diagonal) matrices. For  $j = 2, \dots, m-1$ ,

$$B_j = \begin{bmatrix} a_{1,j}^W & a_{1,j}^P & a_{1,j}^E & & & \\ & a_{2,j}^W & \ddots & \ddots & & \\ & & \ddots & \ddots & a_{n-1,j}^E & \\ & & & a_{n,j}^W & a_{n,j}^P & a_{n,j}^E \end{bmatrix}_{n \times (n+2)}$$



$$B_1 = \begin{bmatrix} a_{1,1}^P & a_{1,1}^E & & & & \\ a_{2,1}^W & a_{2,1}^P & a_{2,1}^E & & & \\ & a_{3,1}^W & \ddots & \ddots & & \\ & & \ddots & \ddots & a_{n-1,1}^E & \\ & & & a_{n,1}^W & a_{n,1}^P & a_{n,1}^E \end{bmatrix}_{n \times (n+1)}$$

$$B_m = \begin{bmatrix} a_{1,m}^W & a_{1,m}^P & a_{1,m}^E & & & \\ & a_{2,m}^W & \ddots & \ddots & & \\ & & \ddots & \ddots & a_{n-2,m}^E & \\ & & & a_{n-1,m}^W & a_{n-1,m}^P & a_{n-1,m}^E \\ & & & & a_{n,m}^W & a_{n,m}^P \end{bmatrix}_{n \times (n+1)}$$

and  $A_j = [\text{diag}(-a_{1,j}^N, \dots, -a_{n,j}^N)]_{n \times n}$ ,  $C_j = [\text{diag}(-a_{1,j}^S, \dots, -a_{n,j}^S)]_{n \times n}$ .

Without loss of generality, assume that the spatial domain is decomposed into  $p_x \times p_y$  number of sub-domains, where  $p_x$  and  $p_y$  are even and every sub-domain includes  $l_x \times l_y$  number of grid points ( $n = p_x l_x$  and  $m = p_y l_y$ ). Also, assume that the sweeping direction of the first sub-domain is *NE-to-SW* at the starting iteration. It is easy to show that the coefficient matrix  $A$  admits the following decomposition (notice that the natural row-wise ordering is considered here),

$$A = G_1 + \beta I + G_2, \quad (6.7)$$

where  $I$  denotes an  $n \times m$  identity matrix here,

$$G_1 = \begin{bmatrix} N_1 & & & \\ & S_2 & & \\ & & \ddots & \\ & & & N_{p_y-1} \\ & & & & S_{p_y} \end{bmatrix}, \quad G_2 = \begin{bmatrix} S_1 & & & \\ & N_2 & & \\ & & \ddots & \\ & & & S_{p_y-1} \\ & & & & N_{p_y} \end{bmatrix},$$

for  $q = 1, \dots, p_y - 1$ ,

$$N_q = \begin{bmatrix} H_{(q-1)l_y+1} & P_{(q-1)l_y+1} & & & \\ & H_{(q-1)l_y+2} & P_{(q-1)l_y+2} & & \\ & & \ddots & \ddots & \\ & & & \ddots & P_{ql_y-l} \\ & & & & H_{ql_y} & P_{ql_y} \end{bmatrix}_{l_y \times (l_y+1)},$$

for  $q = 2, \dots, p_y$ ,

$$S_q = \begin{bmatrix} Q_{(q-1)l_y+1} & V_{(q-1)l_y+1} & & & \\ & Q_{(q-1)l_y+2} & V_{(q-1)l_y+2} & & \\ & & \ddots & \ddots & \\ & & & Q_{ql_y-1} & \ddots \\ & & & & Q_{ql_y} & V_{ql_y} \end{bmatrix}_{l_y \times (l_y+1)},$$

$$N_{p_y} = \begin{bmatrix} H_{(p_y-1)l_y+1} & P_{(p_y-1)l_y+1} & & \\ & \ddots & \ddots & \\ & & H_{p_y l_y-1} & P_{p_y l_y-l} \\ & & & H_{p_y l_y} \end{bmatrix}_{l_y \times l_y},$$

$$S_1 = \begin{bmatrix} V_1 & & & \\ Q_2 & V_2 & & \\ & \ddots & \ddots & \\ & & Q_{l_y} & V_{l_y} \end{bmatrix}_{l_y \times l_y},$$

where  $P_j = A_j$  (for  $j = 1, \dots, m-1$ ),  $Q_j = C_j$  (for  $j = 2, \dots, m$ ) and for  $j = 1, \dots, m$ ,

$$H_j = \begin{bmatrix} NE_{1,j} & & & \\ & NW_{2,j} & & \\ & & \ddots & \\ & & & NE_{p_x-1,j} & \\ & & & & NW_{p_x,j} \end{bmatrix},$$

$$V_j = \begin{bmatrix} SW_{1,j} & & & \\ & SE_{2,j} & & \\ & & \ddots & \\ & & & SW_{p_x-1,j} & \\ & & & & SE_{p_x,j} \end{bmatrix},$$

denoting  $a_{i,j}^{NE} = a_{i,j}^E + a_{i,j}^N$ , for  $r = 1, \dots, p_x - 1$ ,  $j = 1, \dots, m$ ,

$$NE_{r,j} = \begin{bmatrix} a_{(r-1)l_x+1,j}^{NE} & -a_{(r-1)l_x+1,j}^E & & & \\ & a_{(r-1)l_x+2,j}^{NE} & -a_{(r-1)l_x+2,j}^E & & \\ & & \ddots & \ddots & \\ & & & a_{rl_x-1,j}^{NE} & -a_{rl_x-1,j}^E \\ & & & & a_{rl_x,j}^{NE} & -a_{rl_x,j}^E \end{bmatrix}_{l_x \times (l_x+1)}$$

denoting  $a_{i,j}^{NW} = a_{i,j}^W + a_{i,j}^N$ , for  $r = 2, \dots, p_x$ ,  $j = 1, \dots, m$ ,

$$NW_{r,j} = \begin{bmatrix} -a_{(r-1)l_x+1,j}^W & a_{(r-1)l_x+1,j}^{NW} & & & \\ & -a_{(r-1)l_x+2,j}^W & a_{(r-1)l_x+2,j}^{NW} & & \\ & & \ddots & \ddots & \\ & & & -a_{rl_x-1,j}^W & a_{rl_x-1,j}^{NW} \\ & & & & -a_{rl_x,j}^W & a_{rl_x,j}^{NW} \end{bmatrix}_{l_x \times (l_x+1)}$$

denoting  $a_{i,j}^{SW} = a_{i,j}^W + a_{i,j}^S$ , for  $r = 2, \dots, p_x - 1, j = 1, \dots, m$ ,

$$SW_{r,j} = \begin{bmatrix} -a_{(r-1)l_x+1,j}^W & a_{(r-1)l_x+1,j}^{SW} & & & & \\ & -a_{(r-1)l_x+2,j}^W & a_{(r-1)l_x+2,j}^{SW} & & & \\ & & & \ddots & & \\ & & & & \ddots & \\ & & & & & -a_{rl_x-1,j}^W & a_{rl_x-1,j}^{SW} \\ & & & & & -a_{rl_x,j}^W & a_{rl_x,j}^{SW} \end{bmatrix}_{l_x \times (l_x+1)}$$

denoting  $a_{i,j}^{SE} = a_{i,j}^E + a_{i,j}^S$ , for  $r = 2, \dots, p_x - 1, j = 1, \dots, m$ ,

$$SE_{r,j} = \begin{bmatrix} a_{(r-1)l_x+1,j}^{SE} & -a_{(r-1)l_x+1,j}^E & & & & \\ & a_{(r-1)l_x+2,j}^{SE} & -a_{(r-1)l_x+2,j}^E & & & \\ & & & \ddots & & \\ & & & & \ddots & \\ & & & & & a_{rl_x-1,j}^{SE} & -a_{rl_x-1,j}^E \\ & & & & & a_{rl_x,j}^{SE} & -a_{rl_x,j}^E \end{bmatrix}_{l_x \times (l_x+1)}$$

Considering effects of boundaries,

$$SW_{1,j} = \begin{bmatrix} a_{1,j}^{SW} & & & & \\ -a_{2,j}^W & a_{2,j}^{SW} & & & \\ & & \ddots & & \\ & & & -a_{l_x-1,j}^W & a_{l_x-1,j}^{SW} \\ & & & -a_{l_x,j}^W & a_{l_x,j}^{SW} \end{bmatrix}_{l_x \times l_x}$$

$$SE_{p_x,j} = \begin{bmatrix} a_{n-l_x+1,j}^{SE} & -a_{n-l_x+1,j}^E & & & \\ & a_{n-l_x+2,j}^{SE} & -a_{n-l_x+2,j}^E & & \\ & & & \ddots & \\ & & & & a_{n-1,j}^{SE} & -a_{n-1,j}^E \\ & & & & a_{n,j}^{SE} \end{bmatrix}_{l_x \times l_x}$$

Note that matrices  $N_q$  and  $S_q$  should be assembled in  $G_1$  and  $G_2$  such that  $H_j$  and  $V_j$  entries are matched on the corresponding main diagonals. in the same manner,

matrices  $NE_{r,j}$ ,  $NW_{r,j}$ ,  $SE_{r,j}$  and  $SW_{r,j}$  should be assembled in  $H_j$  and  $V_j$  such that their positive diagonals are matched on the corresponding main diagonals.

Using the same approach, parallel sweeping along the other diagonal,  $NW$ -to- $SE$ , implies the following decomposition,

$$A = G_3 + \beta I + G_4, \quad (6.8)$$

Since there is a clear analogy between decompositions (6.7) and (6.8), we avoid further details about  $G_3$  and  $G_4$  too save the space. In fact, during a  $NE$ -to- $SW$  sweep, matrices  $G_1$  and  $G_2$  respectively include the implicit and explicit parts of the computational molecule related to the discretized diffusion operator. During a  $SW$ -to- $NE$  sweep, the position of implicit and explicit parts will be reversed.

To simplify the proof of convergence, we define some helpful matrices and mention their elegant properties here.

**DEFINITION 6.6.** *Multilevel matrix splitting:* Consider  $n \times n$  matrix  $A$  and integer set  $\Xi = \{m_1, m_2, \dots, m_s\}$  such that  $1 \leq s \leq n$ ,  $m_i \geq 1$  ( $i = 1, \dots, s$ ) and  $\sum_{i=1}^s m_i = n$ . The multilevel splitting of matrix  $A$  under set  $\Xi$  which is denoted by  $MLS_{\Xi}(A)$  is defined as set  $\{A_1, A_2, \dots, A_s\}$  such that every matrix  $A_i$  is composed from the first  $m_i$  row and columns of matrix  $A_{i-1}$  ( $i = 1, \dots, s$ ), where  $A_0 = A$ .

**DEFINITION 6.7.** *Alternatively lower-upper triangular matrix:* An  $n \times n$  matrix  $A$  is called alternatively lower-upper triangular, if there is a multilevel splitting set  $\Xi = \{m_1, \dots, m_s\}$  such that every  $A_i \in MLS_{\Xi}(A)$  is either a lower triangular matrix or an upper triangular matrix.

**DEFINITION 6.8.** *Alternatively block lower-upper triangular matrix:* An  $n \times n$  matrix  $A$  is called alternatively block lower-upper triangular, if there is a multilevel splitting set  $\Xi = \{m_1, \dots, m_s\}$  such that every  $A_i \in MLS_{\Xi}(A)$  is either a block lower triangular matrix or a block upper triangular matrix.

**COROLLARY 6.9.** Assume that  $n \times n$  matrix  $A$  is an alternatively lower-upper triangular matrix, then  $\det(A) = \prod_{i=1}^n a_{ii}$  and the set eigenvalues of matrix  $A$  are equal to set of diagonal entries.

*Proof.* The proof is evidently followed considering the definition of the matrix determinant.  $\square$

**COROLLARY 6.10.** Assume that  $n \times n$  matrix  $A$  is an alternatively block lower-upper triangular matrix, then  $\det(A)$  is equal to the product of determinant of its diagonal blocks and the set eigenvalues of matrix  $A$  are equal to union of set of eigenvalues corresponding to the diagonal blocks.

**LEMMA 6.11.** Assume that  $n \times n$  matrix  $A$  is an alternatively lower-upper triangular matrix, then there is a set of permutations with cardinality  $m \leq n$  that maps  $A$  to either a lower triangular or an upper triangular matrix.

**LEMMA 6.12.** Assume that  $n \times n$  matrix  $A$  is an alternatively block lower-upper triangular matrix, then there is a set of permutations with cardinality  $m \leq n$  that maps  $A$  to either a lower block triangular an upper triangular matrix. Since Lemma 6.11 and 6.12 do not play any role in the course of our analysis, we leave

their proof to interested readers.

COROLLARY 6.13. *Matrices  $G_1$ ,  $G_2$ ,  $G_3$  and  $G_4$  in (6.7) and (6.8) are alternatively block lower-upper triangular.*

*Proof.* The proof is evident, considering the structures of  $G_1$ ,  $G_2$ ,  $G_3$  and  $G_4$  illustrated in this section.  $\square$

It is worth mentioning that the same result is hold for sub-matrices  $H_j$  and  $V_j$  which is summarized in the following corollary.

COROLLARY 6.14. *Matrices  $H_j$  and  $V_j$  ( $j = 1, \dots, m$ ), are alternatively block lower-upper triangular.*

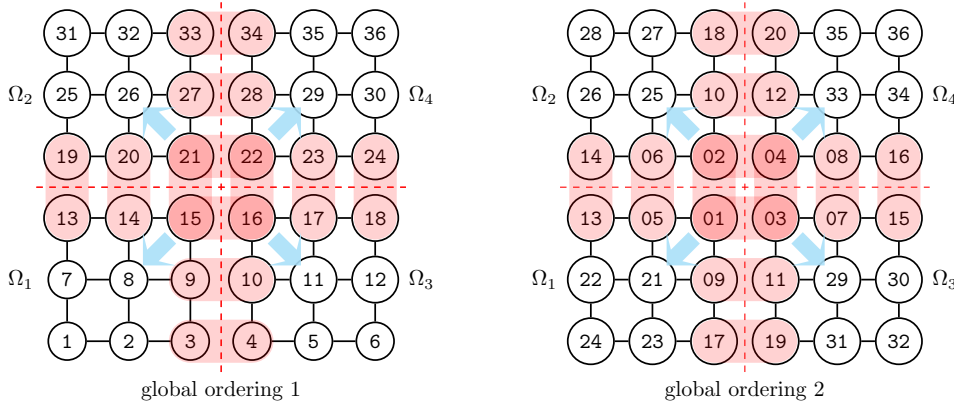


FIG. 6.1. *Decomposition of a  $6 \times 6$  Cartesian mesh into  $2 \times 2$  array of sub-domains: sweeping directions and global order of updating for natural row-wise ordering (left) and parallel sweeping ordering (right).*

Lets to visualize results of Lemma 6.12 and Corollary 6.13 through a simple example. For this purpose we use  $2 \times 2$  decomposition of the  $6 \times 6$  spatial grid shown in left side of figure 3.3. To show the global sparsity pattern, we should first convert local indexing into a global one. We use two type of global ordering here. The first one based on natural row-wise ordering (cf. left hand side of figure 6.1). The second one is globalization of update order according to our algorithm. Assuming local updating index of a node  $\#n$  is in  $\Omega_j$  is denoted by  $i_l$ , its global index is computed as  $i_g = 4 * (i_l - 1) + j$  for coupling nodes and the remaining nodes are indexed based on priority of their domain ID (cf. right hand side of figure 6.1). The global sparsity pattern of  $A$ ,  $G_1$  and  $G_2$  for these two case of global ordering is shown in figure 6.2. The plot clearly confirms the results of corollary 6.13. It is worth mentioning that, the global ordering based on the presented parallel sweeping algorithm defines a permutation to map the alternatively block lower-upper triangular matrices  $G_1$  and  $G_2$  to their corresponding block lower (upper) triangular (compare upper and lower part of figure 6.2).

Assume that eigenvalues of matrices  $G_1$ ,  $G_2$ ,  $G_3$  and  $G_4$  in (6.7) and (6.8) are denoted by the following vectors vectors respectively

$$\Lambda_1 = [\lambda_1^1, \lambda_2^1, \dots, \lambda_n^1]^T, \quad \Lambda_2 = [\lambda_1^2, \lambda_2^2, \dots, \lambda_n^2]^T,$$

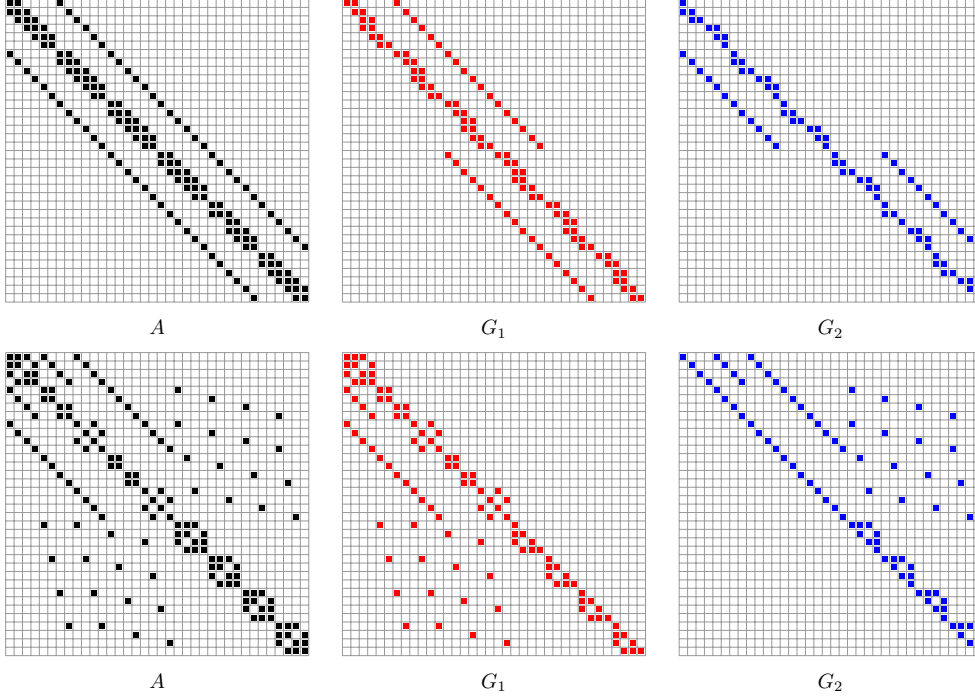


FIG. 6.2. Decomposition of a  $6 \times 6$  Cartesian mesh into  $2 \times 2$  array of sub-domains: global sparsity pattern of  $A$ ,  $G_1$  and  $G_2$  for global ordering based on natural row-wise ordering (up) and parallel sweeping ordering (bottom); cf. figure 6.1.

$$\Lambda_3 = [\lambda_1^3, \lambda_2^3, \dots, \lambda_n^3]^T, \quad \Lambda_4 = [\lambda_1^4, \lambda_2^4, \dots, \lambda_n^4]^T.$$

The following Lemma computes these values explicitly.

LEMMA 6.15. *The following relation holds for sets of eigenvalues of  $G_1$ ,  $G_2$ ,  $G_3$  and  $G_4$  in (6.7) and (6.8),*

$$\Lambda_1, \Lambda_2, \Lambda_3, \Lambda_4 \subset \{ a_{i,j}^{NE}, a_{i,j}^{NW}, a_{i,j}^{SE}, a_{i,j}^{SW} \mid i = 1, \dots, n; j = 1, \dots, m \}.$$

*Proof.* Considering Corollary 6.13, the eigenvalues of  $G_1$ ,  $G_2$ ,  $G_3$  and  $G_4$  are equal to their diagonal entries. The diagonal entries are equal to diagonals of  $H_i$  and  $V_j$  for  $j = 1, \dots, m$  which complete the proof.  $\square$

COROLLARY 6.16. *Matrices  $G_1$ ,  $G_2$ ,  $G_3$  and  $G_4$  in (6.7) and (6.8) are strictly positive definite.*

THEOREM 6.17. *The presented parallel two-dimensional algorithm is convergent if the following condition holds,*

$$|1 - \omega_{SW}| |1 - \omega_{SE}| |1 - \omega_{NW}| |1 - \omega_{NE}| < 1.$$

*Proof.* Let's to define the following temporary notations to concise expressions,

$$\omega_1 \stackrel{\text{def}}{=} \omega_{NE}, \quad \omega_2 \stackrel{\text{def}}{=} \omega_{SW}, \quad \omega_3 \stackrel{\text{def}}{=} \omega_{NW}, \quad \omega_4 \stackrel{\text{def}}{=} \omega_{SE}.$$

Inspiring from the 1D analysis, we consider every four iterations of the presented method as a group of iterations (sweeping along *NE*-to-*SW*, *SW*-to-*NE*, *NW*-to-*SE* and *SE*-to-*NW* respectively). Considering the decomposition (6.7) and (6.8) of  $A$ , we can write the presented two-dimensional parallel iterative algorithm in the following matrix form ( $k = 0, 4, \dots$ ),

$$\begin{aligned}
\left( (\mathbf{a} - \omega_1 \Lambda_1)I + \omega_1 G_1 \right) \mathbf{u}^{(k+1)} &= \left( ((1 - \omega_1)\mathbf{a} + \omega_1 \Lambda_2)I - \omega_1 G_2 \right) \mathbf{u}^{(k)} + \omega_1 \mathbf{f}, \\
\left( (\mathbf{a} - \omega_2 \Lambda_2)I + \omega_2 G_2 \right) \mathbf{u}^{(k+2)} &= \left( ((1 - \omega_2)\mathbf{a} + \omega_2 \Lambda_1)I - \omega_2 G_1 \right) \mathbf{u}^{(k+1)} + \omega_2 \mathbf{f}, \\
\left( (\mathbf{a} - \omega_3 \Lambda_3)I + \omega_3 G_3 \right) \mathbf{u}^{(k+3)} &= \left( ((1 - \omega_3)\mathbf{a} + \omega_3 \Lambda_4)I - \omega_3 G_4 \right) \mathbf{u}^{(k+2)} + \omega_3 \mathbf{f}, \\
\left( (\mathbf{a} - \omega_4 \Lambda_4)I + \omega_4 G_4 \right) \mathbf{u}^{(k+4)} &= \left( ((1 - \omega_4)\mathbf{a} + \omega_4 \Lambda_3)I - \omega_4 G_3 \right) \mathbf{u}^{(k+3)} + \omega_4 \mathbf{f},
\end{aligned} \tag{6.9}$$

where vector  $\mathbf{a}$  includes diagonal entries of  $A$  with an order consistent to  $G_i$ . From (6.9) we have,

$$\mathbf{u}^{(k+4)} = T \mathbf{u}^{(k)} + \bar{\mathbf{f}}, \quad k = 0, 4, \dots \tag{6.10}$$

where,

$$\begin{aligned}
T &= \left( (\mathbf{a} - \omega_4 \Lambda_4)I + \omega_4 G_4 \right)^{-1} \left( ((1 - \omega_4)\mathbf{a} + \omega_4 \Lambda_3)I - \omega_4 G_3 \right) \\
&\quad \times \left( (\mathbf{a} - \omega_3 \Lambda_3)I + \omega_3 G_3 \right)^{-1} \left( ((1 - \omega_3)\mathbf{a} + \omega_3 \Lambda_4)I - \omega_3 G_4 \right) \\
&\quad \times \left( (\mathbf{a} - \omega_2 \Lambda_2)I + \omega_2 G_2 \right)^{-1} \left( ((1 - \omega_2)\mathbf{a} + \omega_2 \Lambda_1)I - \omega_2 G_1 \right) \\
&\quad \times \left( (\mathbf{a} - \omega_1 \Lambda_1)I + \omega_1 G_1 \right)^{-1} \left( ((1 - \omega_1)\mathbf{a} + \omega_1 \Lambda_2)I - \omega_1 G_2 \right)
\end{aligned} \tag{6.11}$$

With some simple manipulations of iteration matrix  $T$ , we have,

$$\tilde{T} = (G_{1-}) (G_{1+})^{-1} (G_{2-}) (G_{2+})^{-1} (G_{3-}) (G_{3+})^{-1} (G_{4-}) (G_{4+})^{-1} \tag{6.12}$$

such that  $\rho(T) = \rho(\tilde{T})$ , and,

$$G_{1+} = (\mathbf{a} - \omega_1 \Lambda_1)I + \omega_1 G_1, \quad G_{1-} = ((1 - \omega_2)\mathbf{a} + \omega_2 \Lambda_1)I - \omega_2 G_1$$

$$G_{2+} = (\mathbf{a} - \omega_2 \Lambda_2)I + \omega_2 G_2, \quad G_{2-} = ((1 - \omega_1)\mathbf{a} + \omega_1 \Lambda_2)I - \omega_1 G_2$$

$$G_{3+} = (\mathbf{a} - \omega_3 \Lambda_3)I + \omega_3 G_3, \quad G_{3-} = ((1 - \omega_4)\mathbf{a} + \omega_4 \Lambda_3)I - \omega_4 G_3$$

$$G_{4+} = (\mathbf{a} - \omega_4 \Lambda_4)I + \omega_4 G_4, \quad G_{4-} = ((1 - \omega_3)\mathbf{a} + \omega_3 \Lambda_4)I - \omega_3 G_4$$

Assume eigenvalues of  $G_{1-}$ ,  $G_{1+}$ ,  $G_{2-}$ ,  $G_{2+}$ ,  $G_{3-}$ ,  $G_{3+}$ ,  $G_{4-}$  and  $G_{4+}$  are denoted by vectors  $\Lambda_{1-} = \{\lambda_i^{1-}\}$ ,  $\Lambda_{1+} = \{\lambda_i^{1+}\}$ ,  $\Lambda_{2-} = \{\lambda_i^{2-}\}$ ,  $\Lambda_{2+} = \{\lambda_i^{2+}\}$ ,  $\Lambda_{3-} = \{\lambda_i^{3-}\}$ ,

$\Lambda_{3+} = \{\lambda_i^{3+}\}$ ,  $\Lambda_{4-} = \{\lambda_i^{4-}\}$  and  $\Lambda_{4+} = \{\lambda_i^{4+}\}$  (for  $i = 1, \dots, mn$ ) respectively, it is easy to show that,

$$\Lambda_{1-} = (1 - \omega_2)\mathbf{a}, \quad \Lambda_{1+} = \mathbf{a}, \quad \Lambda_{2-} = (1 - \omega_1)\mathbf{a}, \quad \Lambda_{2+} = \mathbf{a},$$

$$\Lambda_{3-} = (1 - \omega_4)\mathbf{a}, \quad \Lambda_{3+} = \mathbf{a}, \quad \Lambda_{4-} = (1 - \omega_3)\mathbf{a}, \quad \Lambda_{4+} = \mathbf{a}.$$

Therefore, we have ( $\|\cdot\|$  denotes the Euclidean norm),

$$\begin{aligned} \|\tilde{T}\| &\leq \|(G_{1-}) (G_{1+})^{-1}\| \|(G_{2-}) (G_{2+})^{-1}\| \|(G_{3-}) (G_{3+})^{-1}\| \|(G_{4-}) (G_{4+})^{-1}\| \\ &= \left( \max_{1 \leq i \leq n} \left| \frac{\lambda_i^{1-}}{\lambda_i^{1+}} \right| \right) \left( \max_{1 \leq i \leq n} \left| \frac{\lambda_i^{2-}}{\lambda_i^{2+}} \right| \right) \left( \max_{1 \leq i \leq n} \left| \frac{\lambda_i^{4-}}{\lambda_i^{3+}} \right| \right) \left( \max_{1 \leq i \leq n} \left| \frac{\lambda_i^{4-}}{\lambda_i^{4+}} \right| \right) \\ &= |1 - \omega_2| |1 - \omega_1| |1 - \omega_4| |1 - \omega_3|. \end{aligned} \quad (6.13)$$

Since,  $\rho(T) = \rho(\tilde{T}) = \|\tilde{T}\|$ , using (6.13), the following condition ensures the convergence of iterations:  $|1 - \omega_1| |1 - \omega_2| |1 - \omega_3| |1 - \omega_4| < 1$ .  $\square$

**COROLLARY 6.18.** *The presented two-dimensional parallel Gauss-Seidel algorithm ( $\omega_{NE} = \omega_{SW} = \omega_{NW} = \omega_{SE} = 1$ ) is unconditionally convergent.*

**COROLLARY 6.19.** *When  $\omega_{NE} = \omega_{SW} = \omega_{NW} = \omega_{SE} = \omega$  the convergence criterion of the presented two-dimensional parallel SOR algorithm is similar to that of sequential SOR method, i.e.,  $0 < \omega < 2$ . Moreover, in this case  $\omega_{opt} = 1$ .*

**7. Extension to general structured n-diagonal matrices.** Using the Cartesian tensor product properties of structured grids and following the same procedure mentioned in the previous sections, the extension of our method to three (or higher) spatial dimensions is straightforward. Therefore, it is not of value to further discuss on this issue. Now, let us to generalize our method a bit more.

**DEFINITION 7.1.** (*Cartesian grid*) *The spatial network  $Z \subset \mathbb{R}^d$  ( $d \geq 1$ ) is called as a Cartesian grid in  $\mathbb{R}^d$  if it is formed by tensor product of  $d$  one-dimensional spatial grids.*

**DEFINITION 7.2.** (*Structured grid*) *The spatial network  $Z \subset \mathbb{R}^d$  ( $d \geq 1$ ) is called as a structured grid in  $\mathbb{R}^d$  if there is an orientation preserving deformation in  $\mathbb{R}^d$  which maps  $Z$  to a Cartesian grid in  $\mathbb{R}^d$ .*

It is clear that every structured grid in  $\mathbb{R}^d$  has  $2^d$  corner points and so  $2^d$  directed diagonal directions (sweeping directions in our algorithm).

**DEFINITION 7.3.** (*Structured n-diagonal matrix*) *Consider the following assumptions:  $Z \subset \mathbb{R}^d$  is structured grid with  $m_i$  grid points ( $i = 1, \dots, d$ ) along each spatial dimension. Every grid point of  $Z$  has an ID number based on a natural row-wise ordering.  $A$  is a square matrix with cardinality  $n = \prod_{i=1}^d m_i$ .  $A$  is an  $n$ -diagonal matrix with a symmetric sparsity pattern ( $n$  is odd). Then we called  $A$  as a structured  $n$ -diagonal matrix if there is a computational molecule  $M$  which maps nonzero entries of every row  $i$  of  $A$  to a set of points in the neighborhood of node  $i$  in  $Z$ ; and vice*



*versa.*

We assume that the reader is aware from the required special treatment at/near boundaries of  $Z$ . Therefore, these issues are ignored within Definition 7.3. In fact by Definition 7.3 we would like to extend application of our method to every matrix  $A$  which can be connected to a structured grid, e.g., it can be raised from discretization of a PDE on a structured grid.

Now, we want to generalize previous results, i.e., solving (preconditioning) system of linear equations  $A\mathbf{u} = \mathbf{f}$  by parallel SOR (or ILU) when  $A$  is an irreducible diagonal dominant structured  $n$ -diagonal matrix. Let us briefly mention the outline of algorithm in this case. Assume  $Z \subset \mathbb{R}^d$  is the corresponding structured grid to  $A$ . We first decompose  $Z$  into parts (based on load balancing criteria) and define the sweeping directions for each sub-domain during the course of each  $2^d$  iterations. Then, order of update for coupling points are determined; note that the coupling points are determined based on the current sweeping direction and the computational molecule. Finally the iterative procedure is started by updating coupling points in the corresponding order and then internal nodes. Now let us re-state the convergence theories for this general case. Although, we do not prove the following results, their proof should be straightforward (though can be very massive if one does not find an appropriate abstraction in this regard).

**THEOREM 7.4.** *Consider irreducible diagonal dominant structured  $n$ -diagonal matrix  $A$  with the corresponding structured grid  $Z \subset \mathbb{R}^d$ . The following results hold.*

- (i) *Matrix admit  $(2^d)/2$  decomposition in the following form such that every decomposition correspond to parallel sweeping along an appropriate diagonal of  $Z$ :  $A = G_j + D + G_{j+1}$  for  $j = 1, 3, \dots, d-1$ , where  $D$  is a diagonal matrix with nonnegative entries, for  $i = 1, \dots, d$ , each  $G_i$  is strictly positive definite alternatively block lower-upper triangular matrix with eigenvalues equal to main diagonal.*
- (ii) *Assume that for  $i = 1, \dots, d$ ;  $\omega_i$  denotes the relaxation parameter along the  $i$ -th sweeping direction. Then the presented parallel SOR algorithm is convergent under the following condition:  $\prod_{i=1}^{2^d} |1 - \omega_i| < 1$ .*

**8. Numerical experiment.** In this section we present numerical results on the convergence and performance of the presented method. As the computing platform we used a 32-core machine based on 16 Dual-Core Intel 2400 Mhz nodes (4GB RAM on each node) switched with a Gbit Ethernet network. The MPICH [8] library was used for message passing implementation of exchange algorithm.

The  $d$ -dimensional ( $d = 1, 2, 3$ ) version of following laplace equation is used here as a model problem,

$$\sum_{i=1}^{i=d} \left( \frac{\partial^2 u}{\partial x_i^2} \right) = 0 \quad \text{in } [0, 1]^d, \quad u = \prod_{i=1}^{i=d} x_i \quad \text{on } \partial([0, 1]^d) \quad (8.1)$$

where  $x_i$  denotes the  $i$ -th component of spatial position vector, e.g., for  $d = 3$ ,  $\mathbf{x} = (x_1, x_2, x_3) = (x, y, z)$ . The exact solution of (8.1) is  $\hat{u}(\mathbf{x}) = \prod_{i=1}^{i=d} x_i$ . Since this exact solution is spatially  $d$ -linear, it is possible to recover the exact solution by a spatially second order numerical method, independent of the grid resolution. Therefore, the discretization errors does not contribute in our numerical analysis. In all of our numerical examples in this study, the  $L_1$ -norm of error (with respect to the exact

solution) is used to study the convergence. Assume that the total number of degree of freedoms is  $n$  after the discretization of (8.1), the  $L_1$ -norm of error is computed as follows,  $L_1 - \text{error} = \frac{1}{n} \sum_{l=1}^n |u_l - \hat{u}_l|$ , where  $u_i$  and  $\hat{u}_i$  denote respectively the approximate and exact solutions at the  $i$ -th degree of freedom. Moreover, the initial guess is taken to be  $u_l = 0$  (for  $l = 1, \dots, n$ ) and the iterations is stopped when the  $L_1$ -norm of error is below threshold  $1.e - 3$ ; except in our 3D experiments in which the convergence threshold  $1.e - 2$  is taken into account.

Although we do not plan to release a software related to the presented method, some (crude) Fortran codes related to model problems used in this study are freely available on the following web (mainly to demonstrate the validity of results presented in this section): [http : //sites.google.com/site/rohtav/home/par](http://sites.google.com/site/rohtav/home/par).

**8.1. One-dimensional numerical experiment.** In our one-dimensional numerical experiments (8.1) is solved on uniform grids with resolutions, 41, 81 and 161.

In the first 1D example, the model problem is solved by In this left to right sweeping Gauss-Seidel (LRGS), right to left sweeping Gauss-Seidel (RLGS), symmetric sweeping Gauss-Seidel (SGS) and the presented parallel Gauss-Seidel with various number of sub-domains (PGS(p), p denotes the number of sub-domains).

Table 8.1 shows the results of this experiment. It is clear that the presented method is convergent independent from the number of sub-domains, and the number of iterations to meet the convergence criterion is close to that of the original Gauss-Seidel methods.

TABLE 8.1  
1D parallel Gauss-Seidel vs. 1D sequential Gauss-Seidel.

	41 grids		81 grids		161 grids	
method	iteration	$L_1$ -error	iteration	$L_1$ -error	iteration	$L_1$ -error
LRGS	979	9.94266e-4	3905	9.98916e-4	15598	9.99738e-4
RLGS	960	9.94266e-4	3866	9.98916e-4	15519	9.99738e-4
SGS	976	9.96647e-4	3892	9.99752e-4	15565	9.99977e-4
PGS(2)	975	9.95198e-4	3891	9.99297e-4	15563	9.99825e-4
PGS(4)	974	9.97789e-4	3890	9.99986e-4	15561	9.99779e-4
PGS(6)	974	9.94523e-4	3890	9.99231e-4	15559	9.99769e-4
PGS(8)	973	9.97436e-4	3890	9.98472e-4	15557	9.99807e-4
PGS(10)	973	9.94144e-4	3889	9.99221e-4	15555	9.99809e-4
PGS(14)	972	9.93927e-4	3888	9.99208e-4	15551	9.99755e-4
PGS(18)	970	9.99382e-4	3887	9.99179e-4	15547	9.99783e-4
PGS(24)	-	-	3885	9.99857e-4	15541	9.99814e-4
PGS(30)	-	-	3884	9.99459e-4	15535	9.99738e-4
PGS(36)	-	-	3882	9.99864e-4	15529	9.99704e-4

In the second 1D example the model problem is solved by left to right sweeping SOR (LRSOR), right to left sweeping SOR (RLSOR), symmetric sweeping SOR (SSOR) and the presented parallel SOR with various number of sub-domains (PSOR(p), p denotes the number of sub-domains). The optimal values of  $\omega$  are applied in these experiments. These values are primarily computed via numerical experiments (searching in  $[1.0, 2.0]$  with  $1.e - 3$  accuracy).

Tables 8.2, 8.3 and 8.4 show results of these experiments. According to tables, PSOR method is convergent and has a competitive convergence rate with sequential SOR methods. Since the initial error had an asymmetric spatial distribution, the sweeping directions has considerable effect on the iteration counts. For example RLSOR method has the best convergence rate. Note the presented parallel solver

overcomes LRSOR and SSOR in some cases.

TABLE 8.2  
1D parallel SOR vs. 1D sequential SOR for grid resolution 41.

method	iteration	$L_1$ -error	$\omega_L$ - optimum	$\omega_R$ - optimum
LRSOR	51	9.99298e-4	1.86887	-
RLSOR	31	9.38294e-4	-	1.86637
SSOR	62	9.48613e-4	1.00000	1.87776
PSOR(2)	31	9.46469e-4	1.84970	1.92084
PSOR(4)	76	9.88365e-4	1.00000	1.94890
PSOR(6)	78	9.88246e-4	1.00000	1.94890
PSOR(8)	72	9.85974e-4	1.00000	1.89379
PSOR(10)	71	9.72100e-4	1.00000	1.88577
PSOR(14)	87	9.59733e-4	1.00000	1.95591
PSOR(18)	71	9.60855e-4	1.00000	1.90080

TABLE 8.3  
1D parallel SOR vs. 1D sequential SOR for grid resolution 81.

method	iteration	$L_1$ -error	$\omega_L$ - optimum	$\omega_R$ - optimum
LRSOR	103	9.82824e-4	1.93193	-
RLSOR	61	9.42462e-4	-	1.93143
SSOR	120	8.87046e-4	1.00000	1.93487
PSOR(2)	80	9.54235e-4	1.90982	1.95691
PSOR(4)	164	9.93129e-4	1.00000	1.97194
PSOR(6)	129	9.66998e-4	1.00000	1.96092
PSOR(8)	141	9.91414e-4	1.00000	1.94589
PSOR(10)	140	9.80610e-4	1.00000	1.94088
PSOR(14)	129	9.35418e-4	1.00000	1.95992
PSOR(18)	138	9.96443e-4	1.00000	1.95090
PSOR(24)	141	9.93632e-4	1.00000	1.94790
PSOR(30)	180	9.91055e-4	1.00000	1.97094
PSOR(36)	143	9.91698e-4	1.00000	1.94389

TABLE 8.4  
1D parallel SOR vs. 1D sequential SOR for grid resolution 161.

method	iteration	$L_1$ -error	$\omega_L$ - optimum	$\omega_R$ - optimum
LRSOR	208	9.81709e-4	1.96593	-
RLSOR	122	9.58420e-4	-	1.96493
SSOR	236	9.99534e-4	1.19840	1.96693
PSOR(2)	233	9.82315e-4	1.00000	1.96593
PSOR(4)	342	9.84557e-4	1.00000	1.98497
PSOR(6)	253	9.85584e-4	1.00000	1.97996
PSOR(8)	279	9.72206e-4	1.00000	1.97194
PSOR(10)	277	9.88102e-4	1.00000	1.96994
PSOR(14)	280	9.98979e-4	1.00000	1.96994
PSOR(18)	269	9.91725e-4	1.00000	1.97495
PSOR(24)	277	9.89229e-4	1.00000	1.97395
PSOR(30)	278	9.81003e-4	1.00000	1.96894
PSOR(36)	281	9.73789e-4	1.00000	1.97194

Since the optimal values of  $\omega_L$  in SSOR and PSOR solvers are close to unity, it suggests to apply simultaneous over-relaxation and under-relaxation to improve the convergence. Results of symmetric successive over/under-relaxation SOR (SSOUR) and parallel successive over/under-relaxation SOR (PSOUR) are compared in Table

TABLE 8.5  
1D parallel over/under-relaxation method vs. 1D sequential SOR for grid resolution 41.

method	iteration	$L_1$ -error	$\omega_L$ - optimum	$\omega_R$ - optimum
LRSOR	51	9.99298e-4	1.86887	-
RLSOR	31	9.38294e-4	-	1.86637
SSOUR	58	9.99474e-4	0.24825	1.87087
PSOUR(2)	33	8.68232e-4	1.84785	1.91892
PSOUR(4)	57	9.99032e-4	0.17317	1.87588
PSOUR(6)	57	9.98090e-4	0.11712	1.87387
PSOUR(8)	58	9.99746e-4	0.09910	1.87087
PSOUR(10)	57	9.97719e-4	0.18118	1.87287
PSOUR(14)	52	9.99428e-4	0.36837	1.89590
PSOUR(18)	53	9.98391e-4	0.33233	1.87988

8.5 for grid resolution 41 (the optimal values of relaxation factors are searched in  $[0.0, 2.0]$  with accuracy  $1.e - 3$ ).

**8.2. Two-dimensional numerical experiment.** In our two-dimensional numerical experiments (8.1) is solved by row-wise ordering Gauss-Seidel (RGS) and SOR (RSOR), symmetric Gauss-Seidel (SGS) and SOR (SSOR), frontal sweeping Gauss-Seidel (FGS) and SOR (FSOR) and the presented parallel Gauss-Seidel ( $PGS(p_x, p_y)$ ), where  $p_x$  and  $p_y$  are the number of sub-domains in  $x$  and  $y$  directions respectively) and SOR ( $PSOR(p_x, p_y)$ ) on grid resolutions  $51 \times 51$ ,  $101 \times 101$  and  $151 \times 151$ .

Since the topology of domain decomposition may changes the convergence rate of parallel solver, strip-wise and square-wise topologies are examined in this experiment (cf. figure 8.1). The strip-wise and square-wise domain decompositions have a  $p \times 1$  and  $\sqrt{p} \times \sqrt{p}$  topologies respectively, where  $p$  is the number of sub-domains.

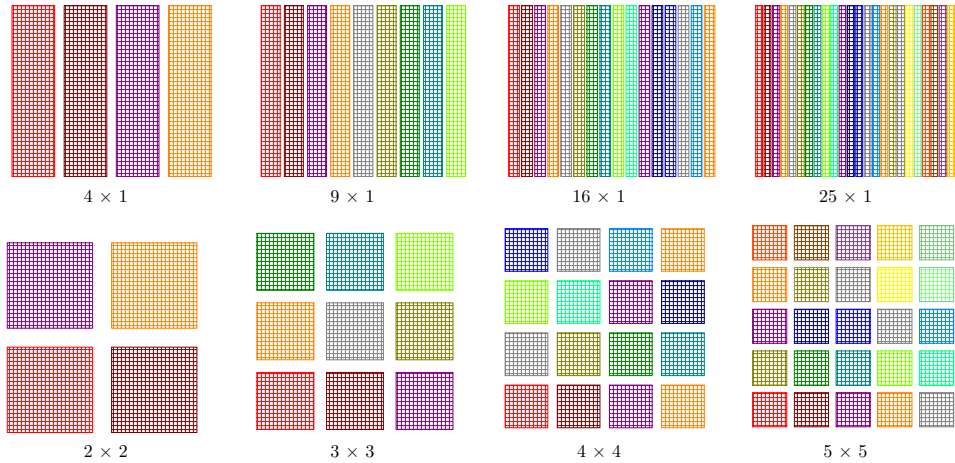


FIG. 8.1. Strip-wise (up) and square-wise (down) sub-domains topologies used in this study.

Results of this experiment are summarized in Tables 8.6, 8.7 and 8.8. According to tables, the number of iterations to meet the convergence for the presented parallel method is close to that of sequential ones, and there is not sensible dependency to the topology of domain decomposition. Note that in this experiment the relaxation parameters for all directions are taken to be equal.

TABLE 8.6  
2D parallel Gauss-Seidel vs. 2D sequential Gauss-Seidel.

grid method	51 × 51		101 × 101		151 × 151	
	iteration	$L_1$ -error	iteration	$L_1$ -error	iteration	$L_1$ -error
RGS	1018	9.98560e-4	4065	9.99123e-4	9139	9.99798e-4
SGS	1006	9.98720e-4	4038	9.99374e-4	9097	9.99960e-4
FGS	1006	9.96308e-4	4037	9.99753e-4	9097	9.99686e-4
PGS(4×1)	1020	9.97194e-4	4066	9.99808e-4	9140	9.99839e-4
PGS(2×2)	1020	9.97652e-4	4065	9.99717e-4	9138	9.99888e-4
PGS(9×1)	1038	9.97011e-4	4103	9.99232e-4	9195	9.99884e-4
PGS(3×3)	1029	9.99224e-4	4082	9.99687e-4	9163	9.99873e-4
PGS(25×1)	1088	9.96490e-4	4219	9.99572e-4	9371	9.99965e-4
PGS(5×5)	1049	9.96392e-4	4116	9.99972e-4	9213	9.99814e-4

TABLE 8.7  
2D parallel SOR vs. 2D sequential SOR. for  $\omega = 1.25$ .

grid method	51 × 51		101 × 101		151 × 151	
	iteration	$L_1$ -error	iteration	$L_1$ -error	iteration	$L_1$ -error
RSOR	616	9.97982e-4	2450	9.99198e-4	5501	9.99339e-4
SSOR	606	9.95519e-4	2425	9.98966e-4	5461	9.99332e-4
FSOR	605	9.95328e-4	2424	9.98924e-4	5460	9.99310e-4
PSOR(4×1)	626	9.95846e-4	2467	9.98854e-4	5524	9.99442e-4
PSOR(2×2)	626	9.98955e-4	2465	9.99991e-4	5521	9.99318e-4
PSOR(9×1)	652	9.96804e-4	2520	9.99830e-4	5605	9.99658e-4
PSOR(3×3)	637	9.99291e-4	2487	9.99869e-4	5556	9.99914e-4
PSOR(16×1)	685	9.94546e-4	2593	9.99467e-4	5718	9.99331e-4
PSOR(4×4)	648	9.98578e-4	2512	9.99153e-4	5590	9.99347e-4
PSOR(25×1)	715	9.94756e-4	2688	9.99302e-4	5863	9.99984e-4
PSOR(5×5)	662	9.94443e-4	2535	9.99867e-4	5624	9.99977e-4

TABLE 8.8  
2D parallel SOR vs. 2D sequential SOR. for  $\omega = 1.5$ .

grid method	51 × 51		101 × 101		151 × 151	
	iteration	$L_1$ -error	iteration	$L_1$ -error	iteration	$L_1$ -error
RSOR	348	9.90645e-4	1373	9.98771e-4	3074	9.99890e-4
SSOR	341	9.88632e-4	1351	9.99049e-4	3038	9.98968e-4
FSOR	339	9.89902e-4	1349	9.99485e-4	3036	9.99170e-4
PSOR(4×1)	369	9.97722e-4	1415	9.98874e-4	3133	9.99910e-4
PSOR(2×2)	369	9.89711e-4	1410	9.98715e-4	3127	9.99310e-4
PSOR(9×1)	407	9.97695e-4	1498	9.97574e-4	3259	9.99389e-4
PSOR(3×3)	382	9.99520e-4	1443	9.97418e-4	3179	9.98991e-4
PSOR(16×1)	453	9.94660e-4	1606	9.96612e-4	3432	9.99365e-4
PSOR(4×4)	396	9.94275e-4	1474	9.99090e-4	3227	9.98820e-4
PSOR(25×1)	477	9.90157e-4	1736	9.99730e-4	3645	9.99353e-4
PSOR(5×5)	407	9.99724e-4	1504	9.98626e-4	3274	9.99382e-4

**8.3. Three-dimensional numerical experiment.** In our three-dimensional numerical experiments (8.1) is solved by row-wise sweeping Gauss-Seidel (RGS) and SOR (RSOR), symmetric sweeping Gauss-Seidel (SGS) and SOR (SSOR), frontal sweeping Gauss-Seidel (FGS) and SOR (FSOR) and the presented parallel Gauss-Seidel ( $\text{PGS}(p_x, p_y, p_z)$ , where  $p_x$ ,  $p_y$  and  $p_z$  are number of sub-domains in x, y and z directions respectively) and SOR ( $\text{PSOR}(p_x, p_y, p_z)$ ) on grid resolutions  $25 \times 25 \times 25$ ,  $51 \times 51 \times 51$  and  $101 \times 101 \times 101$ . Figure 8.2 shows the topologies of domain decompositions used in this numerical experiment. The relaxation parameters are taken to be equal along all sweeping directions in this section.

Table 8.9, 8.10 and 8.11 show results of this numerical experiment. Tables show that the presented parallel 3D solvers are convergent and number of iterations for achieving convergence are close to that of sequential solvers, in particular in some cases the parallel solver performs slightly better than the sequential solver. Like 2D results, the convergence rate of 3D solver has a little dependency to topology of domain decomposition in this experiment.

In contrast to previously suggested parallel SOR methods in literature our results are very promising, as we do not observe sensible convergence decay due to parallelization which is a pathological weakness of alternative parallel SOR methods. This observation suggest us to use the presented parallel SOR solver as a cache efficient SOR method which is disseised in the nest section.

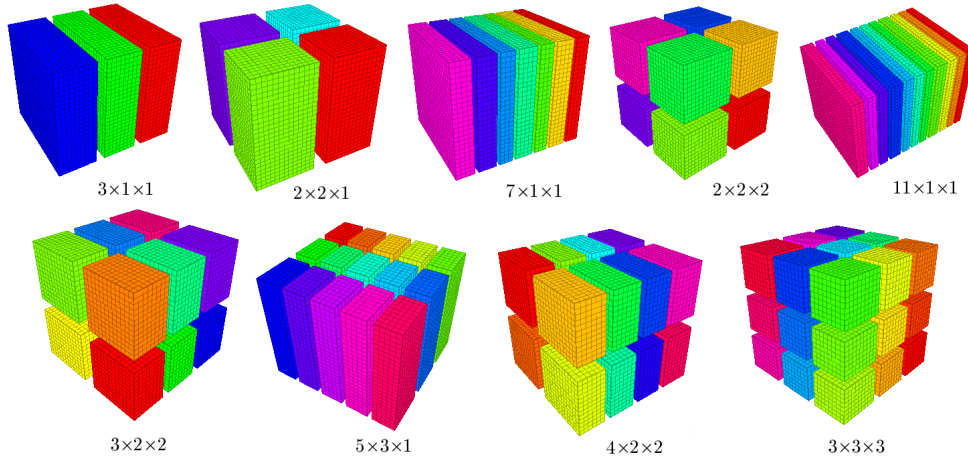


FIG. 8.2. Topologies of domain decompositions in 3D numerical experiment of the present study.

TABLE 8.9  
3D parallel Gauss-Seidel vs. 3D sequential Gauss-Seidel.

grid method	25×25×25		51×51×51		101×101×101	
	iteration	$L_1$ -error	iteration	$L_1$ -error	iteration	$L_1$ -error
RGS	110	9.92077e-3	480	9.96665e-3	1921	9.99432e-3
SGS	104	9.95897e-3	466	9.99655e-3	1893	9.99775e-3
FGS	104	9.86877e-3	466	9.97495e-3	1893	9.99243e-3
PGS(3×3×3)	105	9.96386e-3	468	9.99384e-3	1898	9.99252e-3
PGS(2×2×1)	105	9.99993e-3	469	9.98302e-3	1898	9.99899e-3
PGS(7×1×1)	107	9.87250e-3	472	9.97408e-3	1905	9.99024e-3
PGS(2×2×2)	106	9.93976e-3	470	9.99815e-3	1901	9.99735e-3
PGS(11×1×1)	108	9.92317e-3	475	9.98559e-3	1911	9.99717e-3
PGS(3×2×2)	107	9.92017e-3	472	9.96988e-3	1904	9.99496e-3
PGS(5×3×1)	108	9.94702e-3	474	9.97328e-3	1907	9.99631e-3
PGS(4×2×2)	108	9.83564e-3	473	9.97272e-3	1906	9.99269e-3
PGS(3×3×3)	109	9.91718e-3	475	9.97940e-3	1909	9.99410e-3

TABLE 8.10  
3D parallel SOR vs. 3D sequential SOR. for  $\omega = 1.25$ .

grid method	25×25×25		51×51×51		101×101×101	
	iteration	$L_1$ -error	iteration	$L_1$ -error	iteration	$L_1$ -error
RSOR	69	9.77818e-3	293	9.99745e-3	1164	9.99186e-3
SSOR	63	9.92592e-3	281	9.93894e-3	1137	9.98696e-3
FSOR	62	9.95549e-3	280	9.94525e-3	1136	9.98851e-3
PGS(3×3×3)	65	9.75364e-3	284	9.97072e-3	1144	9.98524e-3
PGS(2×2×1)	65	9.87121e-3	284	9.99866e-3	1144	9.99540e-3
PGS(7×1×1)	67	9.85868e-3	289	9.95523e-3	1154	9.99055e-3
PGS(2×2×2)	66	9.89078e-3	287	9.93992e-3	1149	9.98397e-3
PGS(11×1×1)	69	9.73977e-3	293	9.99839e-3	1164	9.99148e-3
PGS(3×2×2)	67	9.96697e-3	288	9.98010e-3	1152	9.99076e-3
PGS(5×3×1)	68	9.81936e-3	291	9.95989e-3	1157	9.99021e-3
PGS(4×2×2)	68	9.84237e-3	290	9.95890e-3	1155	9.99221e-3
PGS(3×3×3)	69	9.90408e-3	292	9.99708e-3	1159	9.99217e-3

TABLE 8.11  
3D parallel SOR vs. 3D sequential SOR. for  $\omega = 1.5$ .

grid method	25×25×25		51×51×51		101×101×101	
	iteration	$L_1$ -error	iteration	$L_1$ -error	iteration	$L_1$ -error
RSOR	41	9.82565e-3	169	9.97880e-3	659	9.99566e-3
SSOR	36	9.90569e-3	157	9.95554e-3	633	9.97890e-3
FSOR	35	9.57206e-3	155	9.99694e-3	631	9.98964e-3
PGS(3×3×3)	39	9.58539e-3	162	9.93716e-3	643	9.99297e-3
PGS(2×2×1)	38	9.81012e-3	162	9.99555e-3	644	9.99660e-3
PGS(7×1×1)	41	9.90818e-3	170	9.90995e-3	659	9.99539e-3
PGS(2×2×2)	40	9.87981e-3	166	9.95387e-3	651	9.99802e-3
PGS(11×1×1)	44	9.61852e-3	178	9.90053e-3	675	9.99266e-3
PGS(3×2×2)	41	9.72949e-3	169	9.93594e-3	655	9.98725e-3
PGS(5×3×1)	42	9.84760e-3	172	9.90824e-3	662	9.98893e-3
PGS(4×2×2)	42	9.66169e-3	170	9.93732e-3	660	9.97495e-3
PGS(3×3×3)	43	9.73555e-3	173	9.92163e-3	664	9.99070e-3

**8.4. Cache-efficient SOR relaxation.** The growing speed gap between processor and memory has led to the development of hierarchical memories and utility of using caches in modern processors [22]. Nowadays the speed of a code depends increasingly on how well the cache structure is exploited in the course of computation. The number of cache misses is recently an important factor parallel to the number of floating point operations (FLOPS), during comparison of numerical algorithms. Unfortunately, it is not easy to a-priori estimate number of cache misses, but it is easy to perform a posteriori analysis [9].

When a program references a memory location, the data in the referenced location and nearby locations are brought into a cache level. Any additional references to data before these are evicted from the cache will be one or two orders of magnitude faster than references to main memory. So increasing the data locality leads to decreasing cache miss and so the computational performance. A program is said to have a good data locality if, most of the time, the computer finds the data referenced by the program in its cache. The locality of a program can be improved by changing the order of computation and/or the assignment of data to memory locations so that references to the same or nearby locations occur near to each other during the program execution [24]. Interested readers are referred to [9, 12, 22, 24] for further details about this topic.

Based on the above discussion, each parallel algorithm based on the domain decomposition concept is potentially a cache efficient algorithm. The presented method in this study decomposes the global data into smaller sub-domains (with more locality), and after getting essential information from neighbor sub-domains at start of each iteration, performs computations in each sub-domain independently. In this section we shall study the performance of presented parallel SOR from the viewpoint of cache efficiency. For this purpose the 3D model problem is solved with the presented parallel Gauss-Seidel method ( $\omega = 1.0$ ) on grid resolutions  $25 \times 25 \times 25$ ,  $51 \times 51 \times 51$ ,  $101 \times 101 \times 101$  and  $151 \times 151 \times 151$  (a single processor is used in this experiment).

Let's the define the efficiency-factor as the ratio of the total CPU time for cache efficient solver to that of classic sequential solver. Figure 8.3 shows variation of efficiency-factor vs. number of sub-domains in this experiment. The plot shows that when the size of global data is sufficiently large (the cache-miss is susceptible), the efficiency-factor is increased with increasing the number of sub-domains (data locality). Note that with increasing the number of sub-domain the number of FLOPS is slightly increased, but due to mentioned effect solver performs superior.

**9. Closing remarks.** In the present study, a new method is developed to parallelize sequential sweeping procedure on structured grids, and is used to parallelize the SOR (and ILU) preconditioning method on structured grids. This method can be considered as a special overlapping domain decomposition which uses a fully parallel multi-frontal sweeping strategy with local coupling at sub-domains's interfaces. The implementation of method in one and two spatial dimensions is discussed in details and its extension to higher dimension is briefly outlined. The application of method then extended to general structured n-diagonal matrices. Using notion of alternatively block upper-lower triangular matrices, the convergence theory is established in general. Our numerical show that the convergence rate of the presented method is close to that of sequential solver. It is indeed a very promising result does not reported for previous parallel versions of SOR to our knowledge (in fact our method does not show sensible convergence rate decay due to parallilization). This result suggest us to use this solver as cache efficient SOR method. Numerical results on this issue also



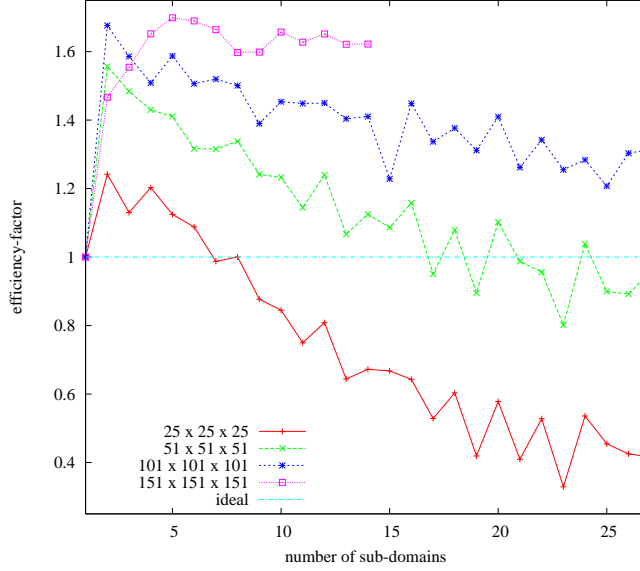


FIG. 8.3. *Parallel SOR as a cache-efficient solver: The variation of efficiency factor vs. number of sub-domains for 3D model problem on grid resolutions  $25^3$ ,  $51^3$ ,  $101^3$  and  $151^3$ .*

support effectiveness of this idea.

It is worth mentioning that our strategy can be directly sued to parallelize other sequential procedures on structured grid. For example in the supplementary material to this work (see: [26]), we use the same strategy to parallelize the fast sweeping method to solve the eikonal equation. The efficiency of that method in some cases (complex geometries) are significantly better than the original fast sweeping as well as classic fast marching method. Moreover in [25], we introduce a fully explicit and unconditionally stable parallel method to solve nonlinear transient heat equation. This method is based on parallelizing multi-dimensional version of the Saul'yev scheme using the presented marching algorithm in this study. Finally, we believe that the presented strategy can be extended to semi-structured grids (like quadtree/octree grids). At the moment, we think that under certain assumptions such an extension is straightforward. Lets to outline this idea on quadtrees. We denote by Cartesian graded quadtree a grid which is resulted from an isotropic hierarchical graded refinement of a square-shaped root cell. Now consider quadtree grid  $\mathcal{Q}$ . Assume there is an orientation preserving deformation  $\mathcal{T}$  which maps  $\mathcal{Q}$  into a graded Cartesian quadtree denoted by  $\hat{\mathcal{Q}}$ . Moreover, assume that there is a square-shaped decomposition<sup>2</sup>  $\mathcal{D}$  on  $\hat{\mathcal{Q}}$  such that every sub-domain is still a graded Cartesian quadtree. Then it is possible to apply the presented parallel strategy on  $\mathcal{D}$ . In this case the sweeping directions within each sub-domain are determined based on  $Z$ -order space filing cures (cf. [6]) started from sub-domain's corners.

**Acknowledgements.** We would like to thanks triple referees for their constructive comments which significantly improve the contents of this paper.

<sup>2</sup>a decomposition with  $\sqrt{p} \times \sqrt{p}$  topology, where  $p$  is number of sub-domains.

## REFERENCES

- [1] L.M. Adams and H.F. Jordan. Is SOR Color-Blind? *SIAM J. Sci. Statist. Comput.*, 7:490, 1986. [1](#)
- [2] L.M. Adams and JM Ortega. A multi-color SOR method for parallel computation. *Proc. 1982 International Conference on Parallel Processing, Bellaire, MI*, pages 53–58, 1982. [1](#)
- [3] Mazzia F. Amodio, P. and. Parallel iterative solvers for boundary value methods. *Math. Comput. Modelling*, 23:2943, 1996. [2](#)
- [4] P. Amodio and F. Mazzia. A parallel Gauss-Seidel method for block tridiagonal linear systems. *SIAM J. Sci. Comput.*, 16(6):1451–1461, 1995. [2](#)
- [5] C.C. Ashcraft and R.G. Grimes. On Vectorizing Incomplete Factorization and SSOR Preconditioners. *SIAM J. Sci. Statist. Comput.*, 9:122, 1988. [1](#)
- [6] MJ Berger, MJ Aftosmis, DD Marshall, and SM Murman. Performance of a new CFD flow solver using a hybrid programming paradigm. *Journal of Parallel and Distributed Computing*, 65(4):414–423, 2005. [33](#)
- [7] U. Block, A. Frommer, and G. Mayer. Block coloring schemes for the SOR method on local memory parallel computers. *Parallel Comput.*, 14:61–75, 1990. [1](#)
- [8] P. Bridges, N. Doss, W. Gropp, E. Karrels, E. Lusk, and A. Skjellum. UsersGuide to mpich, a Portable Implementation of MPI. *Argonne National Laboratory, September*, 1995. [25](#)
- [9] C.C. Douglas, J. Hu, M. Kowarschik, U. Rude, and C. Weiss. Cache Optimization for Structured and Unstructured Grid Multigrid. *Electron. Trans. Numer. Anal.*, 10:21–40, 2000. [32](#)
- [10] S.C. Eisenstat. Comments on scheduling parallel iterative methods on multiprocessor systems II. *Parallel Comput.*, 11:241–244, 1989. [2](#)
- [11] D.L. Harrar II. Orderings, Multicoloring, and Consistently Ordered Matrices. *SIAM J. Matrix Anal. Appl.*, 14:259–278, 1993. [1](#)
- [12] E.J. Im, K. Yelick, and R. Vuduc. Sparsity: Optimization Framework for Sparse Matrix Kernels. *International Journal of High Performance Computing Applications*, 18(1):135, 2004. [32](#)
- [13] D.P. Leary and R.E. White. Multi-splittings of matrices and parallel solution of linear systems. *SIAM Journal on Algebraic and Discrete Methods*, 6:630–640, 1985. [1](#)
- [14] R. Melhem. Towards efficient implementations of preconditioned conjugate methods on vector supercomputers. *Int. J. Supercomput. Appl.*, 1:70–98, 1987. [1](#)
- [15] R.G. Melhem and K.V.S. Ramarao. Multicolor reordering of sparse matrices resulting from irregular grids. *ACM Trans. Math. Software*, 14(2):117–138, 1988. [1](#)
- [16] N.M. Missirlis. Scheduling parallel iterative methods on multiprocessor systems. *Parallel Comput.*, 5:295–302, 1987. [2](#)
- [17] M. Neumann and RJ Plemmons. Convergence of parallel multisplitting iterative methods for M-matrices. *Linear Algebra Appl.*, 88:559–574, 1987. [1](#)
- [18] W. Niethammer. The SOR method on parallel computers. *Numer. Math.*, 56(2):247–254, 1989. [2](#)
- [19] J.M. Ortega. Orderings for Conjugate Gradient Preconditionings. *SIAM J. Optim.*, 1:565–582, 1991. [1](#)
- [20] Y. Robert and D. Trystram. Comments on scheduling parallel iterative methods on multiprocessor systems. *Parallel Comput.*, 7:253–255, 1988. [2](#)
- [21] Y. Saad. *Iterative methods for sparse linear systems*. SIAM, Philadelphia, second edition edition, 2003. [13](#), [15](#)
- [22] S. Sellappa and S. Chatterjee. Cache-Efficient Multigrid Algorithms. *International Journal of High Performance Computing Applications*, 18(1):115, 2004. [32](#)
- [23] S.A. Stotland and J.M. Ortega. Orderings for parallel conjugate gradient preconditioners. *SIAM J. Sci. Comput.*, 18:854–868, 1997. [1](#)
- [24] M.M. Strout, L. Carter, J. Ferrante, and B. Kreaseck. Sparse Tiling for Stationary Iterative Methods. *International Journal of High Performance Computing Applications*, 18(1):95, 2004. [32](#)
- [25] R. Tavakoli. Parallel implementation of SUTCAST solidification solver. *SUTCAST Technical Report, October*, 2005. [33](#)
- [26] R. Tavakoli. Solution of eikonal equation by parallel fast sweeping method. *preprint*, 2009. [33](#)
- [27] R.E. White. Multisplittings and Parallel Iterative Methods. *Comput. Meth. Appl. Mech. Eng.*, 64:567–577, 1987. [1](#)
- [28] D. Xie. A new block parallel sor method and its analysis. *SIAM J. Sci. Comput.*, 27:2006, 1513–1533. [1](#), [2](#)
- [29] D. Xie and L. Adams. New parallel SOR method by domain partitioning. *SIAM J. Sci. Comput.*, 20:2261–2281, 1999. [1](#), [2](#)